

AD_____

Award Number: DAMD17-02-1-0489

TITLE: Computer-Aided Interval Change Analysis of Microcalcifications on Mammograms for Breast Cancer Detection

PRINCIPAL INVESTIGATOR: Lubomir Hadjiiski, Ph.D.

CONTRACTING ORGANIZATION: University of Michigan
Ann Arbor, Michigan 48109-0904

REPORT DATE: July 2007

TYPE OF REPORT: Final

PREPARED FOR: U.S. Army Medical Research and Materiel Command
Fort Detrick, Maryland 21702-5012

DISTRIBUTION STATEMENT: Approved for Public Release;
Distribution Unlimited

The views, opinions and/or findings contained in this report are those of the author(s) and should not be construed as an official Department of the Army position, policy or decision unless so designated by other documentation.

REPORT DOCUMENTATION PAGE				<i>Form Approved</i> OMB No. 0704-0188	
Public reporting burden for this collection of information is estimated to average 1 hour per response, including the time for reviewing instructions, searching existing data sources, gathering and maintaining the data needed, and completing and reviewing this collection of information. Send comments regarding this burden estimate or any other aspect of this collection of information, including suggestions for reducing this burden to Department of Defense, Washington Headquarters Services, Directorate for Information Operations and Reports (0704-0188), 1215 Jefferson Davis Highway, Suite 1204, Arlington, VA 22202-4302. Respondents should be aware that notwithstanding any other provision of law, no person shall be subject to any penalty for failing to comply with a collection of information if it does not display a currently valid OMB control number. PLEASE DO NOT RETURN YOUR FORM TO THE ABOVE ADDRESS.					
1. REPORT DATE (DD-MM-YYYY) 31-07-2007		2. REPORT TYPE Final		3. DATES COVERED (From - To) 1 JUL 2002 - 30 JUN 2007	
4. TITLE AND SUBTITLE COMPUTER-AIDED INTERVAL CHANGE ANALYSIS OF MICROCALCIFICATIONS ON MAMMOGRAMS FOR BREAST CANCER DETECTION				5a. CONTRACT NUMBER	
				5b. GRANT NUMBER DAMD17-02-1-0489	
				5c. PROGRAM ELEMENT NUMBER	
6. AUTHOR(S) Lubomir Hadjiiski, Ph.D. E-Mail: lhadjisk@umich.edu				5d. PROJECT NUMBER	
				5e. TASK NUMBER	
				5f. WORK UNIT NUMBER	
7. PERFORMING ORGANIZATION NAME(S) AND ADDRESS(ES) University of Michigan Ann Arbor, Michigan 48109-0904				8. PERFORMING ORGANIZATION REPORT NUMBER	
9. SPONSORING / MONITORING AGENCY NAME(S) AND ADDRESS(ES) U.S. Army Medical Research and Materiel Command Fort Detrick, Maryland 21702-5012				10. SPONSOR/MONITOR'S ACRONYM(S)	
				11. SPONSOR/MONITOR'S REPORT NUMBER(S)	
12. DISTRIBUTION / AVAILABILITY STATEMENT Approved for Public Release; Distribution Unlimited					
13. SUPPLEMENTARY NOTES					
14. ABSTRACT The goal of this project is to develop a computer-aided diagnosis (CAD) system for automatic interval change analysis of microcalcification clusters on mammograms. Based on our regional registration method and a search program cluster candidates were detected within the local area on the prior. The cluster on the current image is then paired with the candidates to form true (TP-TP) or false (TP-FP) pairs and a correspondence classifier is designed to reduce the (TP-FP). A temporal classifier (TC) based on current and prior information is used if a cluster is detected in the prior, and a current classifier (CurC) based on current information alone is used if no prior cluster is detected. For the TC an LDA, SVM and NN were used. 175 temporal pairs of mammograms were used for evaluation. The registration stage identified 85% (149/175) of the TP-TP pairs with 15 false matches within the 164 image pairs that had detected clusters. The TC based on LDA, SVM and NN achieved a test Az of 0.83, 0.82, 0.84, respectively, for the 164 pairs for classifying the clusters as malignant or benign. For the 11 clusters without detection on the prior, the test Az by the CurC was 0.72. Eight radiologists participated in an observer study using our CAD. The average Az in estimating the likelihood of malignancy was 0.69 without CAD and improved to 0.75 with CAD(p=0.005).					
15. SUBJECT TERMS Breast Cancer, Computer-aided diagnosis, Screening, Classification, Image Analysis					
16. SECURITY CLASSIFICATION OF:			17. LIMITATION OF ABSTRACT UU	18. NUMBER OF PAGES 55	19a. NAME OF RESPONSIBLE PERSON USAMRMC
a. REPORT U	b. ABSTRACT U	c. THIS PAGE U			19b. TELEPHONE NUMBER (include area code)

(3) Table of Contents

(1)	Front Cover	1
(2)	Standard Form (SF) 298, REPORT DOCUMENTATION PAGE	2
(3)	Table of Contents	3
(4)	Introduction	4
(5)	Body	6
(A)	Database collection of malignant and benign breast microcalcification cases that have multiple examinations	6
(B)	Development of a regional registration technique for localization of a search region for the corresponding microcalcification cluster on the prior mammogram of the same view	6
(C)	Adapt automated detection method for identification of candidates of microcalcification clusters within the search region	11
(D)	Development of feature extraction techniques and define similarity measures for matching corresponding microcalcification clusters on current and prior mammograms	13
(E)	Design of a correspondence classifier for identification of matched cluster pairs on current and prior mammograms and eliminate false pairs based on extracted features	14
(F)	Development of feature measures and temporal classifier for characterization of temporal changes in microcalcification clusters	15
(G)	Compare the classification accuracy of the classification scheme using temporal change information with that of a classifier using single-exam information alone	22
(H)	Conduct observer performance study to compare radiologists' classification of malignant and benign microcalcifications with and without the aid of the temporal change classifier	23
(6)	Key research accomplishments in current year as a result of this grant.....	28
(7)	Reportable Outcomes.....	28
(8)	Conclusion	32
(9)	References	34
(10)	Appendix.....	35

(4) Introduction

Treatment of breast cancer at an early stage can significantly improve the survival rate of patients. Mammography is currently the most sensitive method for detecting early breast cancer, and it is also the most practical for screening. Although general rules for differentiation between malignant and benign lesions exist, in clinical practice, approximately only 15-30% of cases referred to surgical biopsy are actually malignant. A number of research groups are in the process of developing computer-aided diagnosis (CAD) methods which can provide a consistent and reproducible second opinion to the radiologist for the detection and classification of breast abnormalities.

Radiologists routinely compare mammograms from a current examination with those obtained in previous years, if available, for identifying interval changes, detecting potential abnormalities, and in evaluating breast lesions. It is widely accepted that interval changes in mammographic features are very useful for both detection and classification of abnormalities. However, CAD techniques that use multiple exams for detection or characterization have not been commonly explored, probably because of the difficulty in the registration of the compressed breast images from different exams. We have been investigating methods for analysis of temporal changes of masses on mammograms to improve detection and classification. To our knowledge, there is no existing CAD technique for registration of microcalcification clusters or classification of microcalcifications based on temporal change information.

The extraction of any meaningful information from a prior mammogram first requires a common frame of reference between the current and prior mammograms. Several complicating factors, such as breast compression difference between current and prior mammograms, energy difference between the two imaging conditions, differences in screen film properties and film processing conditions, and potential changes in breast structures between the two images with patient age, make it difficult to obtain such a frame of reference. On breast images, there are no invariant landmarks (except for the nipple) that can serve as control points in conventional image registration methods to register the two mammograms. In this project, we propose to develop an innovative regional registration method that does not depend on specific control points. We will first approximately align the current and prior mammogram based on maximization of mutual information. Next, we will design a novel approach in which the computer emulates the radiologists' search method in finding corresponding lesions on mammograms. Automated search of microcalcification cluster within the search region on the prior mammogram will be performed. Our current automated microcalcification detection algorithm will provide a basis for this search. However, since the detection is limited to the small search region, the detection can be performed in high resolution and the algorithm parameters can be adjusted to improve the detection sensitivity of the very subtle clusters on the prior mammograms without excessive trade-off in increasing false-positives. A correspondence classifier will be developed to identify the matched pair of clusters on the two mammograms. The image features of the corresponding microcalcification clusters can then be automatically extracted and feature measures characterizing interval changes derived. A classification scheme to differentiate malignant and benign clusters using the interval change information will be developed. This computerized interval change analysis will be an important component of a CAD system for mammographic interpretation.

This project aims at developing a novel interval change analysis scheme to improve the accuracy of CAD. We will investigate the problem of classifying microcalcifications as malignant or benign based on temporal changes in mammographic features using a combination

of computer vision, automated feature extraction, statistical classification, and artificial intelligence techniques. We hypothesize that the use of temporal information would improve the ability of CAD to offer an accurate and objective second opinion to radiologists which, in turn, would increase the positive predictive value of mammography, reduce the number of benign biopsies, and hence reduce both cost and patient morbidity. If integrated in a complete CAD system, the algorithms to be developed in this project may also increase the efficacy of mammography for early detection of breast cancer.

(5) Body

During the duration of this grant (07/01/2002-06/30/2007) we have performed the following studies:

(A) Database collection of malignant and benign breast microcalcification cases that have multiple examinations (Task 1)

We have collected the data set for this study from the files of patients who had undergone biopsy at the University of Michigan. The mammograms are scanned and the images are saved in our storage device using automated graphic user interface developed in our laboratory. Additionally the film information is recorded in a Microsoft Access database. Temporal pairs of images were obtained. The current mammogram of each temporal pair exhibited a biopsy-proven mass. We scan both cranio-caudal (CC) and mediolateral-oblique (MLO) views. The mammograms were digitized with a LUMISCAN 85 laser scanner at a pixel resolution of 0.05 mm x 0.05 mm and with 12-bit resolution.

There were 95 biopsy proven microcalcification clusters (34 malignant and 61 benign) in the 94 cases. The 392 mammograms contained different mammographic views (CC, MLO, and lateral views) and multiple serial examinations of the microcalcification clusters including the examination when the biopsy decision was made. By matching microcalcification clusters of the same view from two different examinations, a total of 261 temporal pairs were formed, of which 94 were malignant and 167 benign.

While the regional registration technique can be used for determining a corresponding structure or region for any structure (both normal tissues and microcalcification cluster) in the breast, in this study we are analyzing its accuracy on biopsy-proven microcalcification cluster alone. The location of the microcalcification cluster on the current mammogram is identified by an Mammography Quality Standards Act (MQSA)-approved radiologist experienced in breast imaging using an interactive image analysis tool on a UNIX workstation. To provide the ground truth for evaluation of the computerized method, the radiologist manually identifies the corresponding region on the prior mammogram. Bounding polygons enclosing the microcalcification cluster on the current mammogram and the corresponding object on the prior mammogram are provided by the radiologist for each case. Each microcalcification cluster as well as the corresponding structure on the prior mammogram are rated for its visibility on a scale of 1 to 10, where the rating of 1 corresponded to the most visible category. The size of the microcalcification cluster on the current mammogram as well as the size of the corresponding structure on the prior mammogram are also measured by the radiologist. The parenchymal density is rated based on the Breast Imaging Reporting and Data System (BI-RADS) lexicon.

(B) Development of a regional registration technique for localization of a search region for the corresponding microcalcification cluster on the prior mammogram of the same view (Task 2)

We have developed a multistage regional registration technique for identifying corresponding microcalcification clusters on temporal pairs of mammograms. This detection approach mimics the method used by radiologists for searching corresponding lesions on mammograms, i.e., the lesion is searched at approximately the same radial distance from the nipple on both views, and feature comparison will be used for further identifying the matching lesion. In the first stage, an initial search region was estimated on the prior mammogram based

on the lesion location on the current mammogram. In the second stage the search region was refined. In the third stage the lesion was detected within the search region.

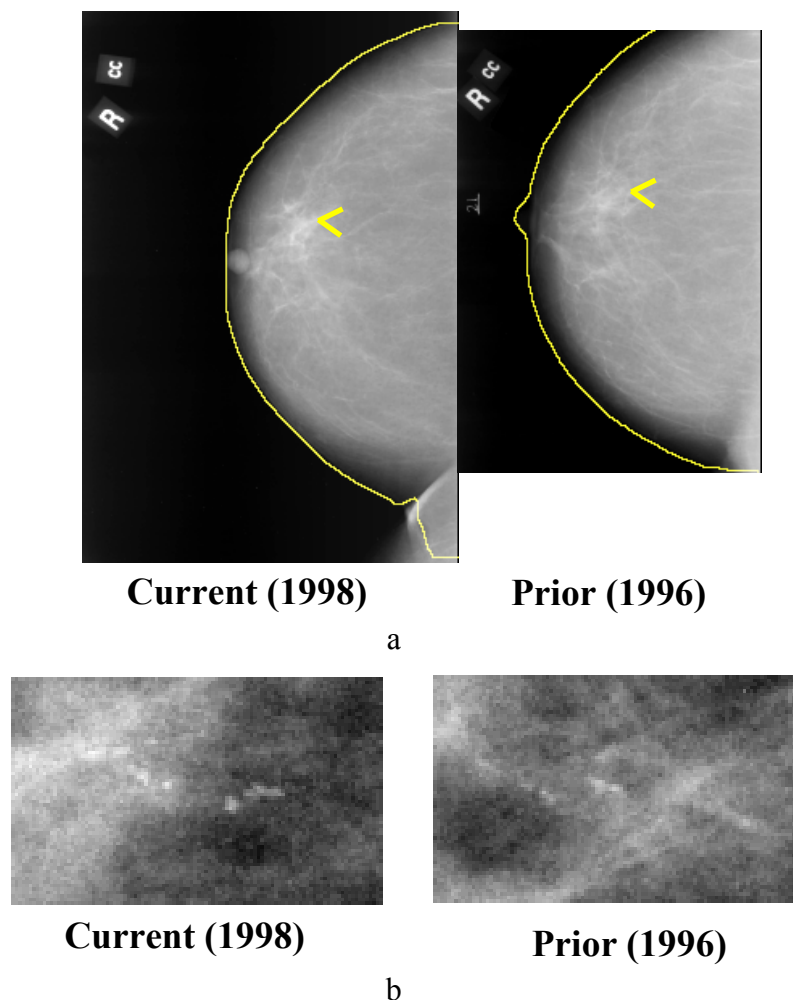


Figure 1. Temporal pair of mammograms containing microcalcification cluster. a) current and prior mammograms with automatically obtained breast outlines, b) current and prior microcalcification cluster.

Initially, the breast image was segmented from the background in the current and prior mammograms (Figure 1). We used the methods already developed in our lab, which work reliably for segmentation of the breast image from the background for our automated detection algorithms for single images [1], [2].

For the first stage of the multistage regional registration technique we need the nipple location on the current and prior mammograms. We are in the process of developing an automated nipple detection program. Currently its accuracy is about 85% in a data set of 744 images (91% for 599 images with visible nipple and 62% for 145 images with invisible nipple) [3]. However, at this time we used manually marked nipple locations on the mammograms. We still need to further improve the accuracy of the nipple detection algorithm in order to use it into the initial step of our automated interval change analysis scheme.

Initial global alignment of mammograms

In the first stage of registration, an initial fan-shaped search region is automatically defined on the prior mammogram based on the cluster location on the current mammogram. The cluster on the current mammogram can either be detected by an automated program or selected interactively by a radiologist. Currently we used the markings of the cluster locations given by the radiologist.

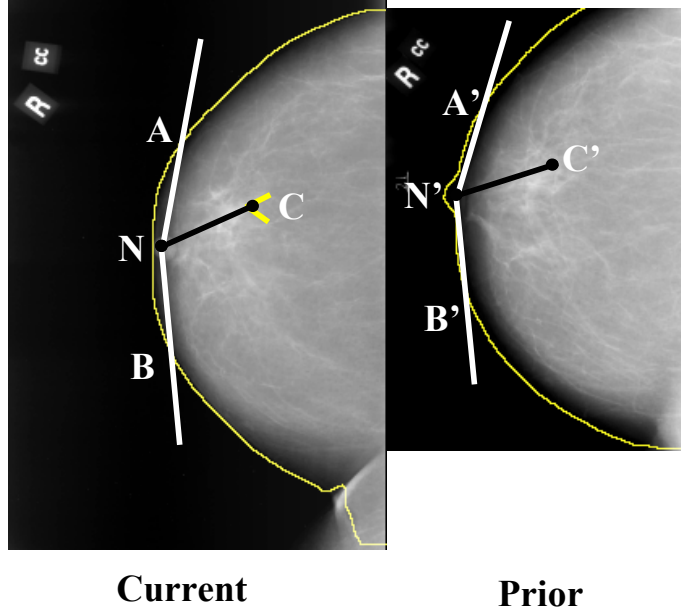


Figure 2. Initial estimation of the cluster centroid position on the prior mammogram based on the nipple-cluster distance and the angle between the nipple-cluster axis and breast periphery on the current mammogram.

For the initial estimation of the lesion centroid location on the prior mammogram, we previously developed a regional registration method (RRM) [4][5], based on the radial distance between the nipple and the lesion centroid and the angular distance between the nipple-lesion centroid axis and the breast boundary on the current mammogram. The location of the microcalcification cluster on the current mammogram is determined in a polar coordinate system with the nipple as the origin. By using the radial distance R_{curr} between the nipple and cluster centroid, $|NC|$, an arc is drawn which intersects the breast boundary at points **A** and **B** (Figure 2). Three angles are estimated at the radial distance R_{curr} : the angle β between **NC** and **NA**, the angle φ between **NC** and **NB**, and the angle θ between **NA** and **NB** ($\theta = \beta + \varphi$). The location of the cluster is determined by R_{curr} and the angle β or φ . The angle θ is the breast width at the radial distance R_{curr} . Using the radial distance R_{curr} to draw an arc centered at the nipple centroid on the prior mammogram, **N'**, the two intersect points **A'** and **B'** with the breast boundary on the prior mammogram are determined. The angle θ_p between the axes $|N'A'|$ and $|N'B'|$ is estimated. An angular scaling factor α can be calculated as the ratio of the prior and the current angles, $\alpha = \theta_p / \theta$. In order to predict the angular location of the microcalcification cluster on the prior mammogram, the smaller angle between β and φ is selected as the angular coordinate of the cluster on the current mammogram. The selected angle, multiplied by the angular scaling

factor α , is used as the predicted angle from the corresponding axis on the prior mammogram. The radial distance R_{curr} is used to predict the radial position of the microcalcification cluster on the prior mammogram.

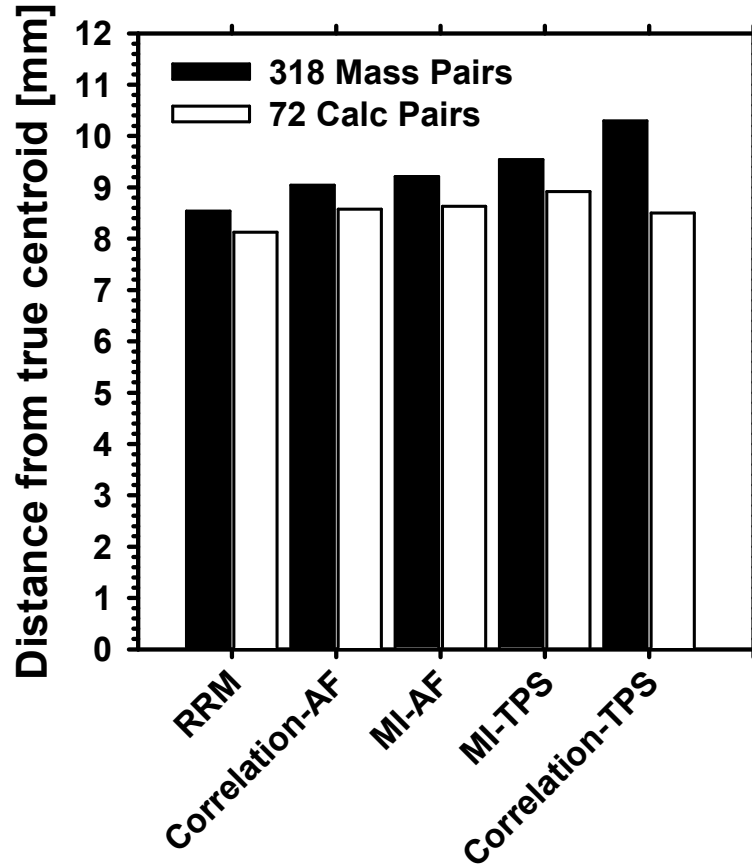


Figure 3. Average distance between the estimated and the true lesion centroids on the prior mammogram for the 5 registration methods: RRM, Correlation-AF, Correlation-TPS, MI-AF, MI-TPS. Seventy two temporal pairs containing microcalcification clusters were used for training the parameters of the warping techniques. The remaining 318 mass pairs were used for testing the performance of the 5 methods.

In this project, the differences in the breast images on the current and prior mammograms were approximately accounted for by warping the current mammogram. We compared both linear and nonlinear global warping of the current mammogram, and studied if these different approaches will improve the localization. In addition we compared the warping techniques to RRM for the initial estimation of the lesion location.

Using the nipple location on both mammograms as an anchor point, the affine (AF) or thin plate splines (TPS) transformation in combination with simplex optimization [6], [7] iteratively warped the current mammogram. The iteration was driven by the maximization of the similarity measure between the breast structures on the current and prior mammograms. Correlation and mutual information (MI) similarity measures were evaluated. An affine

transformation [8] is a linear transformation combining scaling, rotation and translation. The transformed object is linearly resized and rotated. In general, the breast images on the two mammograms are distorted with respect to each other nonlinearly. We therefore also investigated if nonlinear warping functions such as thin-plate splines [9], [10] will provide better alignment between the two images. Thin-plate splines warping based on maximization of mutual information have been used successfully for 3D warping of medical images [11]. We studied if this approach will be effective for 2D alignment of breast images.

A set of 390 temporal pairs of mammograms containing biopsy-proven microcalcification clusters or masses was used. 72 temporal pairs containing microcalcification clusters were used for training the parameters of the warping techniques. The remaining 318 pairs were used for testing the performance of the 5 methods. The registration accuracy was analyzed by evaluating the average distance between the centroids of the estimated and the true lesion locations on the prior mammogram.

We found that the average distance between the estimated and the true lesion centroids on the prior mammogram after the initial stage was: RRM = 8.5 ± 6.2 mm, correlation-AF = 9.0 ± 6.7 mm, correlation-TPS = 10.3 ± 8.2 mm, MI-AF = 9.2 ± 7.5 mm, MI-TPS = 9.5 ± 8.6 mm (Figure 3).

The RRM method outperformed the warping techniques. It localized the corresponding lesions on temporal pairs of mammograms with the highest accuracy and the lowest standard deviation among the 5 methods. These results were presented at RSNA, 2003 [A1]. Based on these results the RRM was selected to be used in our project.

The RRM method was tested additionally on the data set of 175 temporal pairs of mammograms from 65 patients containing biopsy-proven microcalcification clusters. By using the RRM, the average distance between the estimated and the true centroid of the microcalcification clusters on the prior mammogram was 7.95 ± 4.73 mm.

Definition of search region

The location of the cluster on the current mammogram is defined in a polar coordinate system with the nipple as the origin. The position of the microcalcification cluster on the prior mammogram is predicted in a similar manner. An initial fan-shaped search region centered at the predicted location by RRM method from previous stage of the cluster centroid is then defined on the prior mammogram (Figure 4). The size of the fan-shaped region is estimated previously [4][5] to have the form $\epsilon = 0.25 + 5/R_{curr}$ and $\delta = 20$ mm, where ϵ determines the angular width and δ determines the radial length of the fan shaped region. The constants were chosen experimentally on independent mass data set [5] such that the estimated fan-shaped regions will essentially include all masses on the prior mammograms. A fan-shaped template centered at the microcalcification cluster is also defined on the current mammogram. The above defined fan shaped search region was with an average area of 1401 mm^2 and allowed all clusters for the 175 pairs to be within the fan shape search region. The above defined fan shaped search region also allowed all clusters for the enlarged dataset of 261 pairs to be within the fan shape search region.

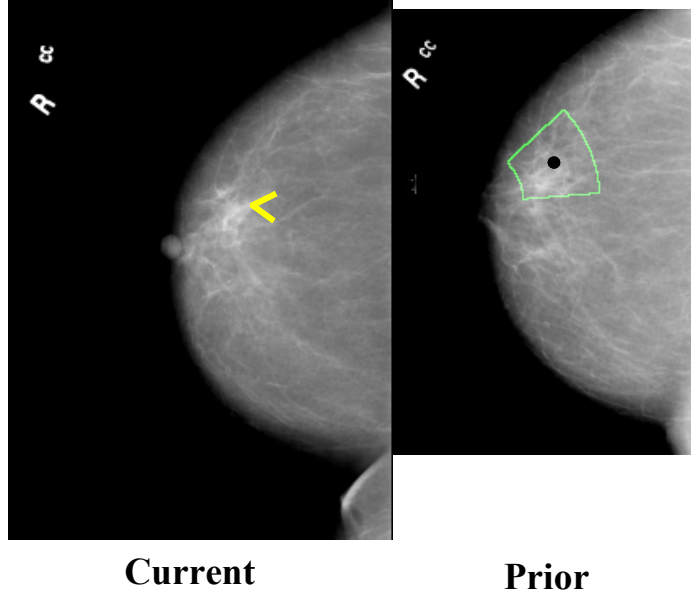


Figure 4. Definition of an initial fan-shape search region on the prior mammogram centered at the predicted centroid location.

(C) Adapt automated detection method for identification of candidates of microcalcification clusters within the search region (Task 3)

We were able to adapt the automatic microcalcification detection to perform efficiently in the task of identification of microcalcification clusters within a small search region. The search region (ROI) estimates the area that the cluster is most likely located but it does not provide the exact location. As the next step, automated detection of microcalcification cluster within the search region is performed. Our current automated microcalcification detection algorithm [12] provides a basis for this search. Since the detection is limited to the small search region, the algorithm parameters can be adjusted to improve the detection sensitivity of the very subtle clusters on the prior mammograms without excessive trade-off in increasing false-positives (FPs).

In the second stage of the registration technique, we investigated the possibility of detection of cluster candidates within the search region with our automated cluster search program with increased sensitivity. We performed tuning of the cluster search program by adjusting the signal to noise threshold (SNR), minimum and maximum values for the number of detected signals, and the neural network output threshold. We observed that with higher values for the minimum and maximum limits for the number of detected signals (i.e. allowing larger number of detected signals), and using higher neural network output threshold we obtained better sensitivity with smaller number of FP.

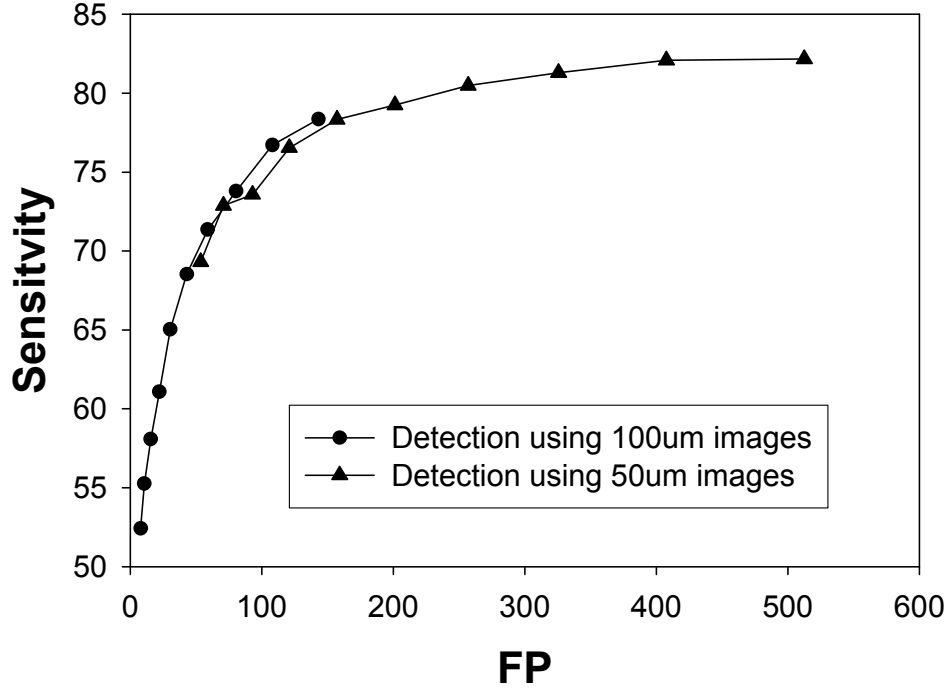


Figure 5. Detection results for the two algorithms optimized to detect microcalcifications on 100um and 50um images respectively. The FP rate is for individual calcs and it is averaged per image.

Using our conventional current cluster detection program with standard thresholds and 100 um images, 76.6% (134/175) of the clusters (TP) with an average of 0.45 false positives (FP) were detected within the search region on the prior mammogram.

Using a high-sensitivity threshold and parameters and 100 um images, the cluster search program detected 89.1% (156/175) of the true clusters (TP) with an average of 0.43 false positives (FP) cluster within the search region on the prior mammograms.

During the past years we have adapted the program to use 50 um images by retraining the parameters of the detection algorithm for 50 um pixel size to optimize its accuracy. The retraining was based on hand selected individual microcalcification locations from experienced medical physicist on 57 prior mammograms.

Using the subset of the 57 prior mammograms with the hand selected individual microcalcification locations we evaluated also the performance of the detection algorithm both for 50 um and 100um mammograms. We selected the set of best parameters for each system. The detection results are presented on Figure 5. We can observe that there was no improvement in the case when we used detection on 50um images in the range of reasonable FP rate (FP per individual microcalcifications).

We continued optimizing the parameters and thresholds for the detection on 100um images. Using an optimized high-sensitivity thresholds and parameters for the 100 um images, the cluster search program detected 90.3% (158/175) of the true clusters (TP) on the priors with an average of 0.43 false positives (FP) cluster within the search region on the prior

mammograms. These results show slight improvement in the detection rate for the cluster search program using 100um images and the optimized set of parameters and thresholds.

The above results are summarized in Table 1.

Table 1. Detection results within the local search area.

Detection type	TP [%]	FP/image
Conventional cluster detection program, Standard thresholds, 100 um image	76.6%	0.45
Cluster search program, High-sensitivity threshold and parameters, 100 um image	89.1%	0.43
Cluster search program, Optimized high-sensitivity threshold and parameters, 100 um image	90.3%	0.43

This results were presented at RSNA 2005 [A4].

In addition, after enlarging our dataset to 261 pairs of current and prior mammograms containing microcalcification clusters, the detection based on the optimized high-sensitivity threshold and parameters on 100 um images was 91.2% (238/261) TP with an average of 0.42 FP cluster within the search region on the prior mammogram.

(D) Development of feature extraction techniques and define similarity measures for matching corresponding microcalcification clusters on current and prior mammograms (Task 4)

The cluster (TP) on the current image was paired with every detected cluster (TP or FP) in the search region to form (TP-TP) and (TP-FP) pairs. Texture and morphological features were extracted from the clusters on the current and the prior mammograms. We extracted morphological features such as area, contrast, axis ratio and eccentricity of an effective ellipse, and moments of the individual microcalcifications and their statistics within a cluster such as the mean, standard deviation, or histogram shape (e.g., skewness and kurtosis). The extracted texture features were calculated from the spatial gray-level dependence (SGLD) matrices [13], and from the gray level difference statistics (GLDS) [14][15]. These texture features describe characteristics such as contrast, local homogeneity, and regularity in the image.

Difference similarity measure was derived from the extracted features of the TP or FP clusters for each temporal pair. We formed the following similarity measures between the current and prior features for each individual feature: the difference, the absolute difference, the squared difference, and the Euclidean distance.

We compared the performance of above similarity measures for the design of the correspondence classifier which is reported in the next section.

We studied a number of similarity measures for the task of template matching of a template containing a current lesion (current mammogram) within the search region on prior mammogram containing the prior lesion. We found that correlation, cosine and Gamma similarity measures outperformed similarity measures such as mutual information. The results of this study

were publicatished in [16] and were presented at IWDM 2004 [17].

In this particular study we also investigated whether the correlation, cosine, and Gamma similarity measures, which showed a great promise for template matching, can be useful in the case of the correspondence classifier. We have performed an extensive testing by designing a number of correspondence classifiers based on these difference features. However the classification results were consistently slightly worth compared to the results of the correspondence classifier based on squared difference features.

We also attempted to design a new type of similarity measure in order to obtain better difference features. A coefficient, σ_{diff} , was computed for each feature as a difference function of both the feature from the current and prior cluster in each pair. The coefficient σ_{diff} , was computed as follows:

$$\sigma_{diff} = \left(\frac{1}{2} \right)^{0.1 * |\sigma_{prior} - \sigma_{current}|},$$

where σ_{prior} and $\sigma_{current}$ are the current and prior features for the particular current-prior temporal pair of candidate clusters.

- (E) **Design a correspondence classifier for identification of matched cluster pairs on current and prior mammograms and eliminate false pairs based on extracted features (Task 5).**

In the final stage, a correspondence classifier was designed to reduce the false pairs (TP-FP) within the search region (Figure 6). We used the above obtained difference similarity measure features as the input to the classifier. A leave-one-case-out training and testing resampling scheme was used for feature selection and classification. A stepwise feature selection with floating window of 5 was used in order to obtain a subset of effective features. We used a linear discriminant classifier to merge the selected features for classification of the TP-TP and TP-FP cluster pairs.

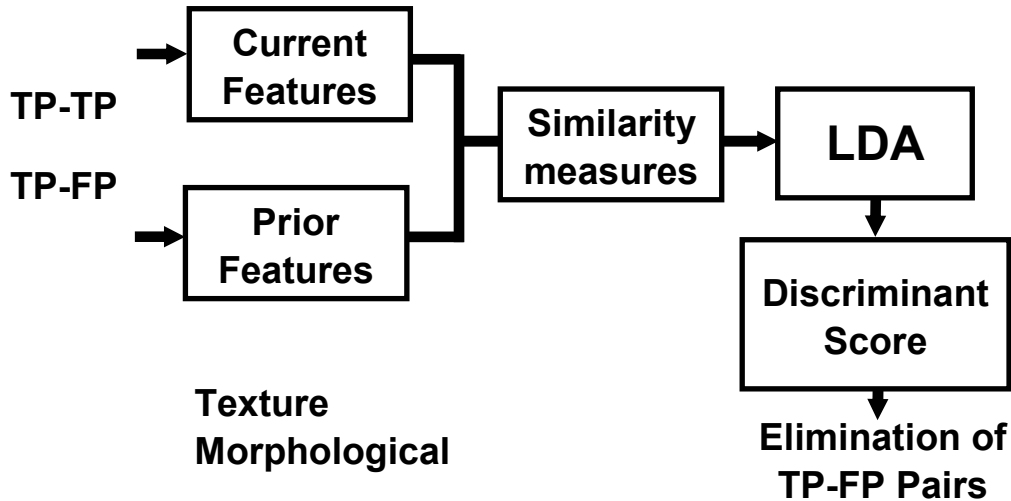


Figure 6. The correspondence classifier designed to reduce the false pairs.

The best result for the correspondence classifier was obtained for a combination of the squared difference morphological features. Six features on average were selected. The test area under ROC curve A_z , for the correspondence classifier was 0.82. The correspondence classifier reduced the FP rate to an average of 0.15 FP cluster with sensitivity of 85% (149/175) (Table 2). This improved result compared to our previous report and study [A2] is due to the improved quality of the morphological features. These results were presented at RSNA 2005 [A4].

Table 2. Results for the correspondence classifier.

Number of features	A_z	TP [%]	FP/image
6	0.82	85%	0.15

For the enlarged dataset of 261 pairs we applied a leave-one-case-out resampling method for feature selection from the set of morphological difference features. The best results were obtained using the difference features based on the difference measure σ_{diff} . An average of 4.3 features were selected per cluster pair. A linear discriminant analysis classifier was applied in leave-one-out training and testing mode applying the selected features for each case. The candidate cluster pair with the highest test discriminant scores was selected. The use of the correspondence classifier yielded 86.6% (226/261) TP-TP pairs with an average FP rate of 0.13 FP cluster. The results from the correspondence classifier are summarized in Table 3.

Table 3. Results for the correspondence classifier based on 261 pairs.

Number of features	A_z	TP [%]	FP/image
4	0.78	87%	0.13

(F) Develop feature measures for characterization of temporal changes in microcalcification clusters and design a classification scheme for differentiation of malignant and benign microcalcifications. (Task 6).

During the duration of this grant we were able to make a major progress in the direction of designing an automatic CAD system for characterization of temporal cases on malignant and benign. This is very novel and unique CAD system which includes an automatic registration of the corresponding current and prior clusters and then classifying them by a temporal classifier on malignant and benign (Figure 7). For this purpose the feature extraction and classification were carried out with the clusters and individual microcalcifications obtained automatically from the registration stage [A1], [A2], [A3], [A4]. The design of an automatic CAD also presents challenges. The automatically detected cluster locations on the temporal pairs may deviate from the optimal locations as selected by expert radiologists. This will introduce “noise” to the extracted features and make the classification task more difficult. In addition for some cases there is no detection on prior mammogram and only current information can be used.

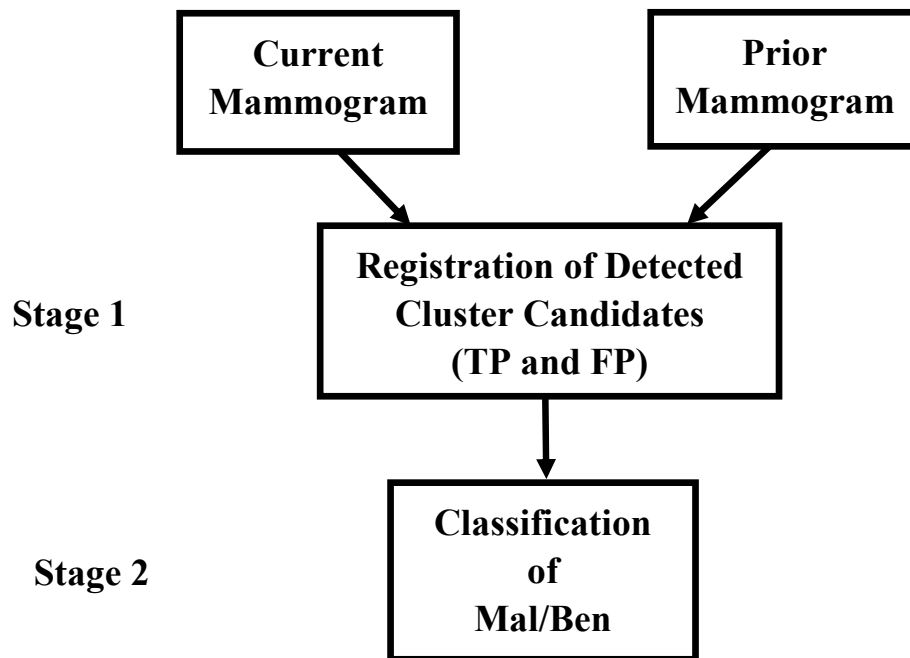


Figure 7. Block-diagram of the registration – classification CAD for temporal microcalcification clusters.

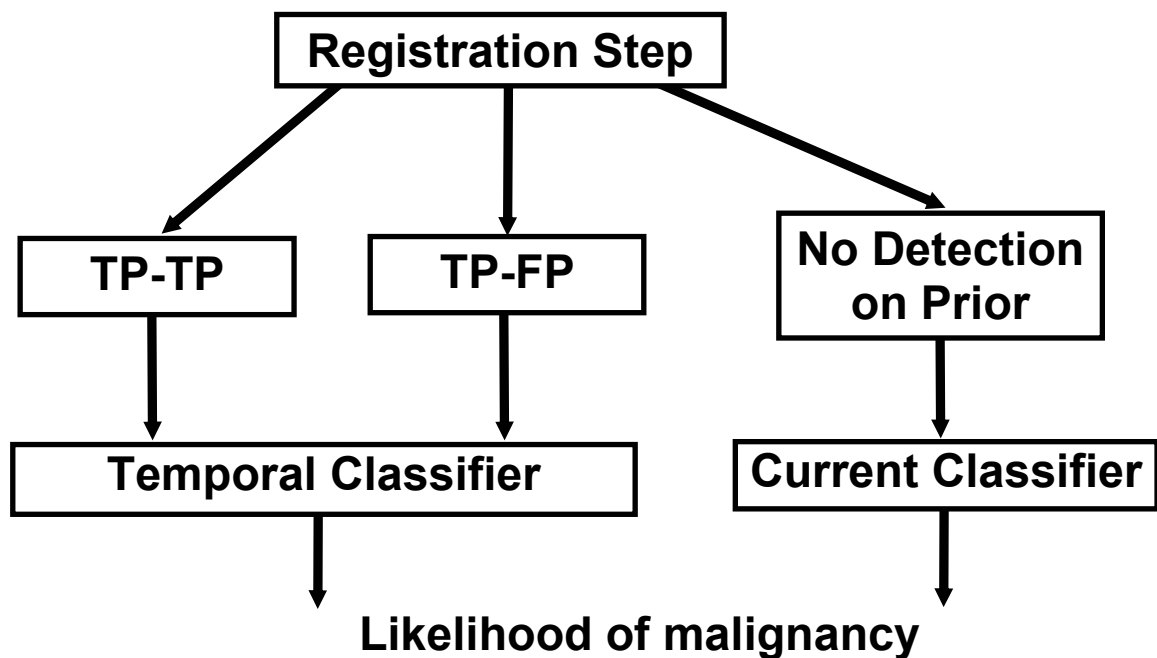


Figure 8. Classification of temporal pairs of microcalcification clusters on malignant and benign combining temporal classifier for the TP-TP and TP-FP pairs and current classifier for the cases without detection on prior.

Feature extraction and definition of difference features

In this study, a new classification scheme using interval change information was developed to classify mammographic microcalcification clusters as malignant and benign [A4] (Figure 8).

From each automatically detected cluster, 20 run length statistic texture features (RLSF) and 21 morphological (Mo) features were extracted [18]. Additionally, 78 SGLD [13] and 64 GLDS [14], [15] texture features were also extracted. All texture features (RLSF, SGLD, and GLDS) were extracted from automatically detected cluster locations. The morphological features were extracted from the automatically detected microcalcifications within the automatically detected cluster locations.

Twenty difference RLSF were obtained by subtracting a prior RLSF from the corresponding current RLSF. We have designed a new feature, the ratio feature, which is defined as the ratio between current and prior feature [16], [A4]. We have obtained 21 Mo ratio features. In addition we used current GLDS features.

Table 4. The feature vector used for the temporal classifier.

Generated feature type	Ratio features	Difference features	Current features
Features	Mo	RLSF	GLDS
Number of features	21	20	64

The feature space consisted of the Mo ratio features, the difference RLSF, as well as the current GLDS features (Table 4).

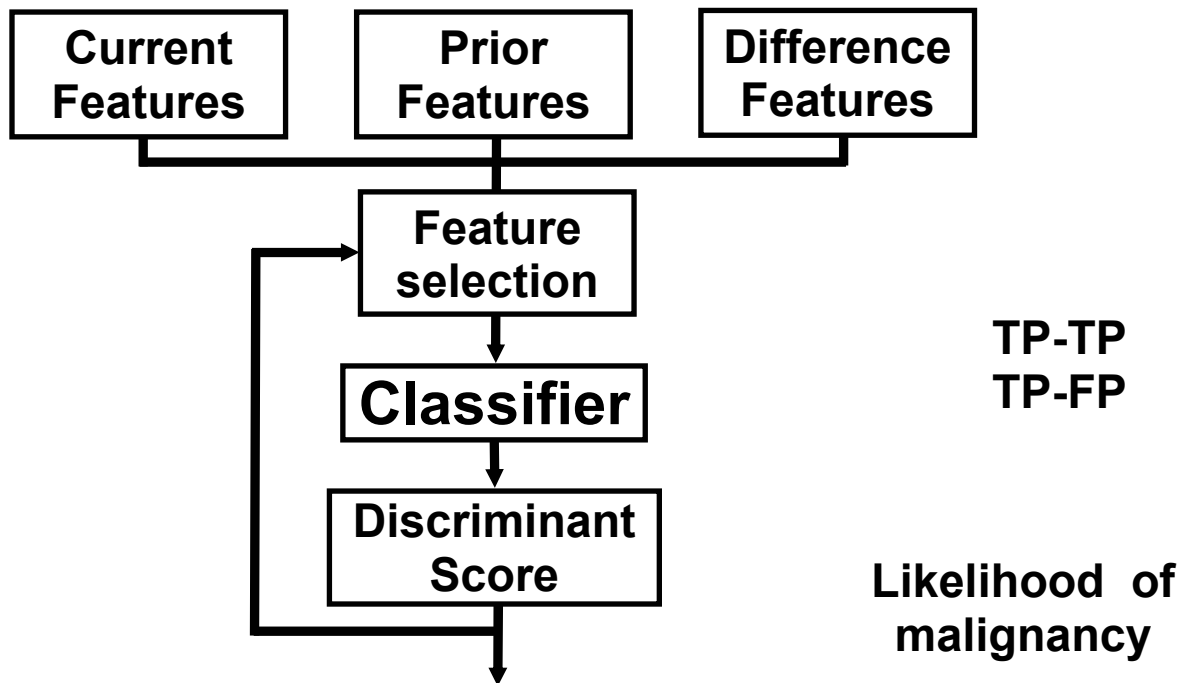


Figure 9. Temporal classifier for classification of temporal pairs of microcalcification clusters on malignant and benign.

Classifier design

When we are designing the classification system for classification of microcalcification clusters on malignant and benign we have to consider the fact that the microcalcification detection algorithm may not be able to detect all clusters on prior. If the cluster is very subtle the automatic microcalcification detection for the identification of microcalcification clusters may not be able to detect it. In this case two types of classifiers are designed (Figure 8). A temporal classifier (Figure 9) based on current and prior information is used if a cluster is detected in the prior, and a current classifier (Figure 12) based on current information alone is used if no prior cluster is detected. The temporal classifier is trained to classify the true (TP-TP) and false (TP-FP) pairs. The automatically detected cluster locations on the temporal pairs may deviate from the optimal locations as selected by expert radiologists. This will introduce “noise” to the extracted features and make the classification task more difficult.

In the past years of the project we have concentrated our efforts on using different types of classification methods in the temporal classifier in order to classify the temporal pair on malignant and benign. We have used a linear discriminant analysis classifier (LDA), support vector machine classifier (SVM) [19] and a multilayer perceptron neural network with backpropagation training (NN). A stepwise feature selection with floating window of 3 were used to select the most useful feature subsets and to merge the feature into a discriminant score (Figure 9). A leave-one-case-out resampling scheme was used for feature selection and to train and to test the classifiers.

In addition a current classifier was trained using the current images from the temporal pairs (the cases that has no detection on prior) and tested on the cases that have not detection on prior (Figure 12). LDA classifier was used in this task. The classification accuracy was analyzed by receiver operating characteristic (ROC) methodology.

In this study, 175 serial pairs containing biopsy-proven calcification clusters were used. On the priors, the radiologist rated 12 of the 175 clusters as not visible and the subtlety of 18 clusters as 9 or 10 on a scale of 10.

At the first stage of the system (Figure 7), 85% (149/175) of the TP-TP pairs were identified with 15 false matches within the 164 image pairs that had computer detected clusters on the priors. Therefore 164 temporal image pairs (149 TP-TP and 15 TP-FP), of which 49 were malignant, were used for classification as malignant and benign. At the second stage (Figure 7), the SVM, LDA and NN temporal classifiers were used for the classification of the 164 cluster temporal pairs.

For each of LDA and SVM (both radial and dot kernel) temporal classifiers a feature selection was performed. Feature selection for NN is a very competitively intensive process and because of this for the NN temporal classifier we used the best feature set obtained for the LDA temporal classifier.

LDA temporal classifier

When an LDA temporal classifier was used the best result was obtained for an average of 7 features selected (Table 5). The selected features included 1 difference RLS feature, 4 morphological ratio features and 2 GLDS features from the current image. All the features were consistently selected for all the training partitions. The LDA temporal classifier achieved test A_z of 0.83 ± 0.03 (Table 7). The A_z results for the LDA temporal classifier with different number of selected features is presented in Figure 10.

Table 5. Selected features for the combined classifier for classification on malignant and benign of automatically detected clusters in current and prior mammograms.

Classifier	Feature type	Ratio features	Difference features	Current features
Temporal classifier LDA, NN	Mo	4		
	RLSF		1	
	GLDS			2
Temporal classifier SVM (dot kernel)	Mo	3		
	RLSF		1	
	GLDS			3
Temporal classifier SVM (radial kernel)	Mo	3		
	RLSF		1	
	GLDS			3

SVM temporal classifier

SVMs with dot kernel, radial kernel and tanh kernel (neural kernel) [19] were studied [C1]. The training and testing results are presented in Table 6.

The SVM temporal classifier with dot kernel achieved training A_z of 0.87 ± 0.03 and test A_z of 0.82 ± 0.03 . The selected features for the dot kernel included 1 difference RLS feature, 3 morphological ratio features and 3 GLDS features from the current image (Table 5). The performance of the SVM with dot kernel for the different number of selected features is presented in Figure 10. For the small number of features the performance of the SVM with dot kernel was close to LDA. However for the larger number of features the LDA slightly overperformed the SVM with dot kernel.

The SVM temporal classifier with radial kernel achieved training A_z of 0.86 ± 0.03 and test A_z of 0.81 ± 0.03 (Table 6). For this kernel the selected features were also 1 difference RLS feature, 3 morphological ratio features and 3 GLDS features from the current image (Table 5). The A_z values of the SVM temporal classifier with radial kernel were consistently smaller than that for the SVM with dot kernel for the different number of features. (Figure 10).

The SVM temporal classifier with tanh kernel (neural kernel) achieved training A_z of 0.86 ± 0.03 and test A_z of 0.82 ± 0.03 (Table 6). However, it required 83 support vectors and it was slower to train. Because of that we did not perform feature selection used the best feature set we had from the LDA classifier.

The SVM with dot kernel performed the best compared to the SVMs with other kernels. It also required the smallest number of support vectors.

NN temporal classifier

A NN with 7 input nodes, different number of neurons in the hidden layer, and 1 output node was used. The NN achieved the best result ($A_z = 0.84 \pm 0.03$) for 8 hidden nodes (Figure 11). The performance of the NN temporal classifier as a function of the number of the hidden neurons is presented in Figure 11. For most of the NN structures the test A_z was 0.83 or lower. For larger number of hidden neurons we have observed slight overtraining. For 8 hidden nodes there was a pick in A_z , which corresponded to the best result.

Table 7 summarizes the results of using different classification methods for the temporal classifier. The difference in A_z between any one of the classifiers did not achieve statistical significance. LDA classifier revealed good stable performance with very simple structure of the

classifier. This was the reason to be selected for the observer study experiment.

In comparison, the MQSA radiologist achieved an A_z of 0.72 ± 0.04 for the 164 temporal pairs.

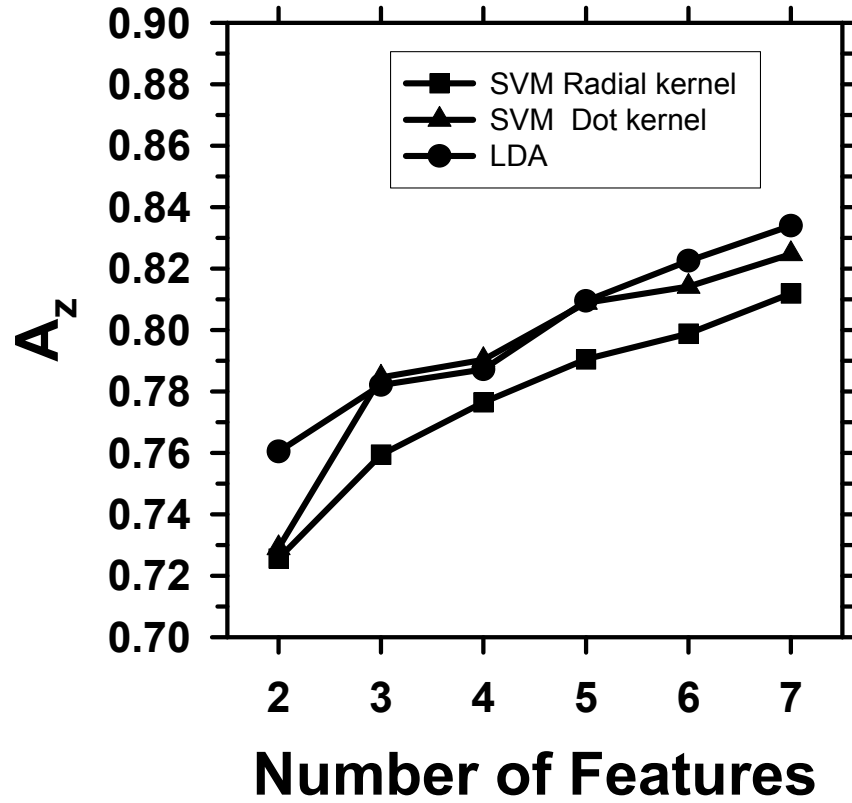


Figure 10. Test A_z results for SVM (radial and dot kernels) and LDA with different number of selected features.

The difference RLS texture features, morphological ratio features and GLDS current features were useful for identification of malignancy in temporal pairs of mammograms. The information on the prior image improved characterization of the microcalcification clusters: 5 out of the 7 selected features contained prior information for the LDA and NN; 4 out of the 7 selected features contained prior information for the SVM.

Table 6. SVM classification results based on 7 selected features.

SVM Type	Training A_z	Test A_z	Number SV
Dot Kernel	0.87 ± 0.03	0.82 ± 0.03	78
Radial Kernel	0.86 ± 0.03	0.81 ± 0.03	89
Tanh Kernel	0.86 ± 0.03	0.82 ± 0.03	83

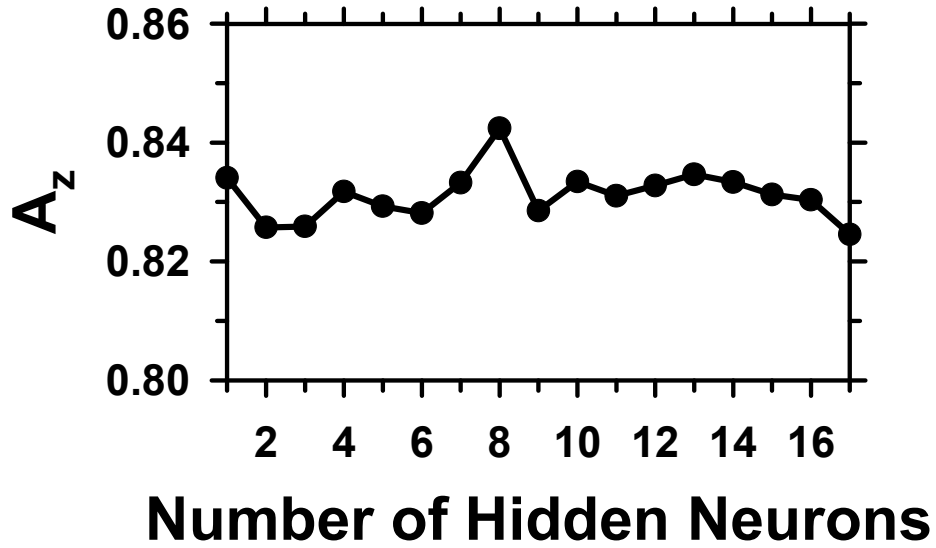


Figure 11. Test results for NN with different number of neurons in the hidden layer.

For the current classifier (Figure12) that was classifying 11 clusters without detection on the prior, an average of 6 features from the current images were selected (Table 8). The selected features included 1 current RLS feature, 3 current morphological features and 2 GLDS current features. All the features were consistently selected for all the training partitions. The test A_z by the current classifier was 0.72 ± 0.14 for classifying the clusters as malignant or benign (Table 9).

Table 7. Overall results for the LDA, SVM, NN classifiers.

	Training A_z	Test A_z
LDA Classifier based on temporal pairs	0.87 ± 0.03	0.83 ± 0.03
SVM Classifier based on temporal pairs	0.87 ± 0.03	0.82 ± 0.03
NN Classifier based on temporal pairs	0.87 ± 0.03	0.84 ± 0.03
LDA Classifier based on current images alone	0.82 ± 0.03	0.76 ± 0.04
MQSA radiologist	-	0.72 ± 0.04

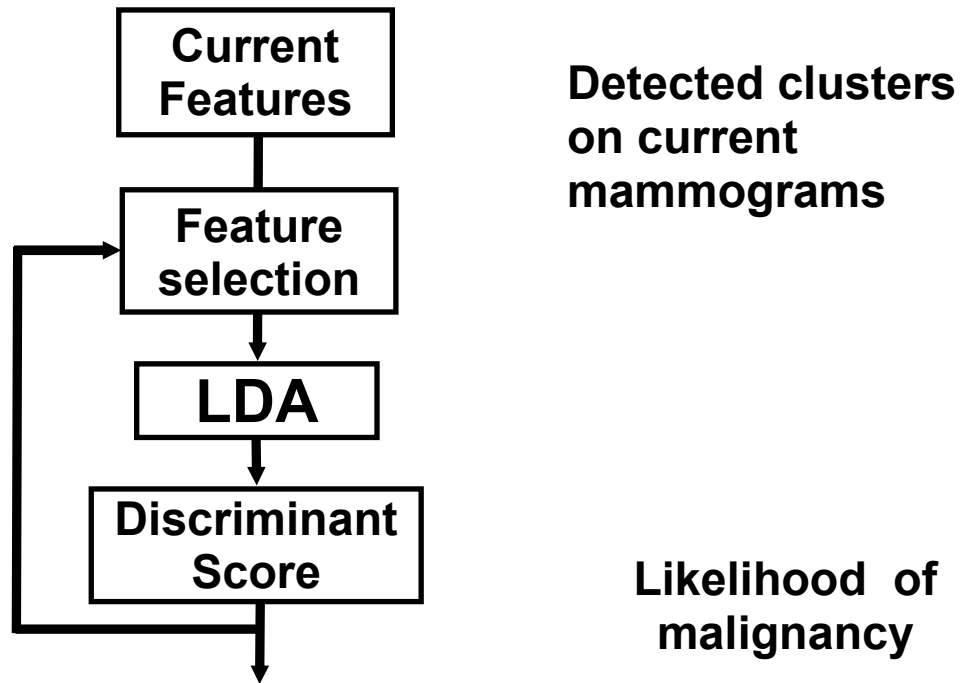


Figure 12. Current classifier based on current information alone. It is used in the case if no prior cluster is detected.

Table 8. Selected features for the combined classifier for classification on malignant and benign of automatically detected clusters in current and prior mammograms.

Classifier	Feature type	Ratio features	Difference features	Current features
Current classifier	Mo			3
	RLSF			1
	GLDS			2

Table 9. Test results for the combined classifier for classification on malignant and benign of automatically detected clusters in current and prior mammograms.

Classifier Type	Temporal classifier	Current classifier
No. of pairs (or only current images)	164	11
Number of selected features	7	6
A_z	0.83 ± 0.03	0.72 ± 0.14

- (G) Compare the classification accuracy of the classification scheme using temporal change information with that of a classifier using single-exam information alone (Task 7)

We have performed a comparison between the temporal classifier and classifier based on current

images (Table 10). For the current classifier an average of 6 features from the current images were selected (Table 5). The selected features included 1 current RLS feature, 3 current morphological features and 2 GLDS current features. All the features were consistently selected for all the training partitions. The test A_z for the classifier based on 164 current images was 0.76 ± 0.04 . For the LDA temporal classifier an average of 7 features were selected (Table 5). The selected features included 1 difference RLS feature, 4 morphological ratio features and 2 GLDS features from the current image. All the features were consistently selected for all the training partitions. We can observe an improvement for the temporal classifier ($A_z = 0.83 \pm 0.03$) when compared to the current classifier ($A_z = 0.76 \pm 0.04$).

Table 10. Results for the combined classifier for classification on malignant and benign of automatically detected clusters in current and prior mammograms.

Classifier Type	Temporal classifier	Current classifier
Number of selected features	7	6
A_z	0.83 ± 0.03	0.76 ± 0.04

We also are in the final stages of preparing a manuscript with above results which will be submitted to the journal of Medical Physics.

(H) Conduct observer performance study to compare radiologists' classification of malignant and benign microcalcifications with and without the aid of the temporal change classifier (Task 8)

We have designed an observer performance experiment with ROC methodology to evaluate the effects of computer classification on radiologists' estimates of the likelihood of malignancy of temporal pairs of microcalcification clusters [A5], [A6], [A7]. A graphical user interface was developed on a PC to display side-by-side the temporal pairs of masses in a predesigned random order for each observer (Figures 13 and 14). The likelihood of malignancy (LM) estimates and the BI-RADS assessment of the radiologist on each pair is automatically recorded when they select it on a slider. The readers provided estimates of the LM and BI-RADS assessments without and then with CAD.

Data set

261 pairs of serial mammograms from 94 patients containing biopsy-proven clustered microcalcifications (94 malignant and 167 benign) were chosen from patient files in our department with IRB approval. The selection criterion was that the case had serial exams in which a corresponding mass can be identified. The microcalcification clusters on both the current and prior mammograms thus encompassed a range of sizes and conspicuity that will be seen in clinical practice. The mammograms were digitized with a LUMISCAN 85 laser scanner at a pixel resolution of $50\mu m \times 50\mu m$ and 4096 gray levels. The image matrix size was reduced by averaging every 2×2 adjacent pixels and down-sampled by a factor of 2 resulting in images with a pixel size of $100\mu m \times 100\mu m$ for further analysis. The true cluster locations on current and prior mammograms were identified by an MQSA radiologist. For each cluster on current mammogram, the corresponding cluster on prior was automatically detected and matched with the current cluster. Regions of interest containing the corresponding clusters were extracted from

the current and prior mammograms of each pair and analyzed by the CAD system. All cases eventually underwent biopsy so that interval change was observed for most of the clusters even if they were found to be benign after biopsy. This was therefore a difficult data set for interval change analysis.

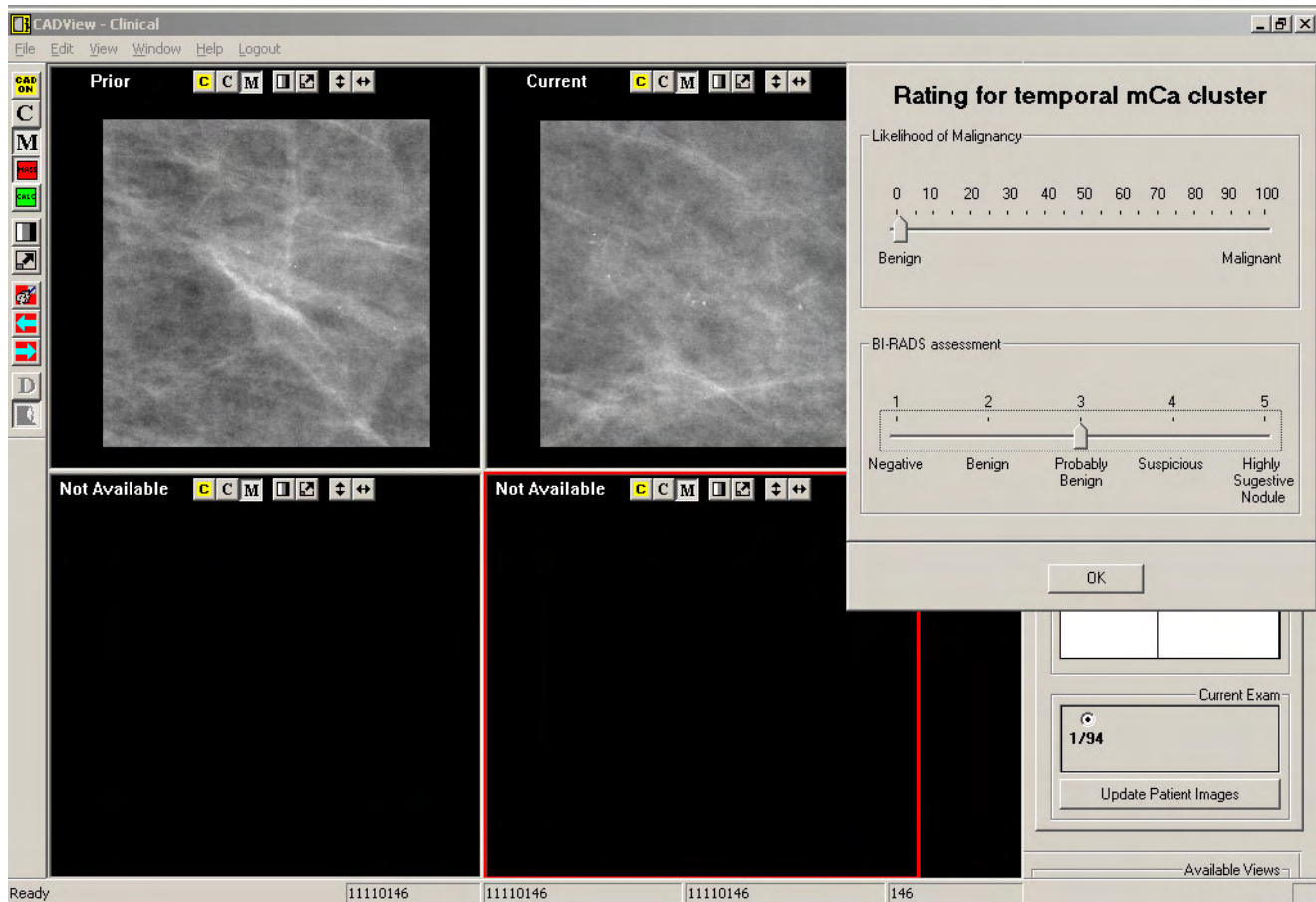


Figure 13. Graphical interface used in the observer study. The example shown was reading in the mode without CAD. The image on the left is prior, the image on the right is current. The radiologist provided two ratings: an estimate of the likelihood of malignancy and the BI-RADS assessment, shown at the upper right area of the screen.

Observer performance study

The observer study evaluated radiologists' performance on the classification of malignant and benign breast masses by interpreting a temporal pair of ROIs containing the mass on a display monitor. The radiologist was asked to provide an estimate of the likelihood of malignancy (LM) on a 0 - 100% scale and the BI-RADS assessment for each mass. The study was designed in "sequential" reading mode in which the radiologist initially read a temporal pair without computer aid, followed by reading the same pair with computer aid. The computer would first record the ratings without computer aid before displaying the computer rating of the mass. The radiologist could change the ratings after taking into consideration the computer rating. Eight MQSA radiologists participated as observers in this study.

A counter-balanced design was used in arranging the reading orders in different modes and the case orders in different reading sessions for the observers. This approach would minimize the potential effects such as learning, fatigue, and memorization on the outcomes of the observer experiments. A graphic user interface was developed for the purpose of presenting the temporal pairs of mass ROIs to the radiologists and recording their ratings (Figures 13 and 14).

Data analysis

The likelihood of malignancy ratings of the individual observers for the different reading conditions were analyzed by using ROC methodology. The classification accuracy was quantified by using the total area under the ROC curve, A_z , as well as the partial area index calculated above a sensitivity threshold of 0.90, $A_z^{(0.90)}$. The area under the ROC curve was estimated by the Dorfman-Berbaum-Metz (DBM) multi-reader multi-case (MRMC) methodology [20]. The statistical significance of the difference of A_z between the different reading conditions was also estimated by the DBM analysis.

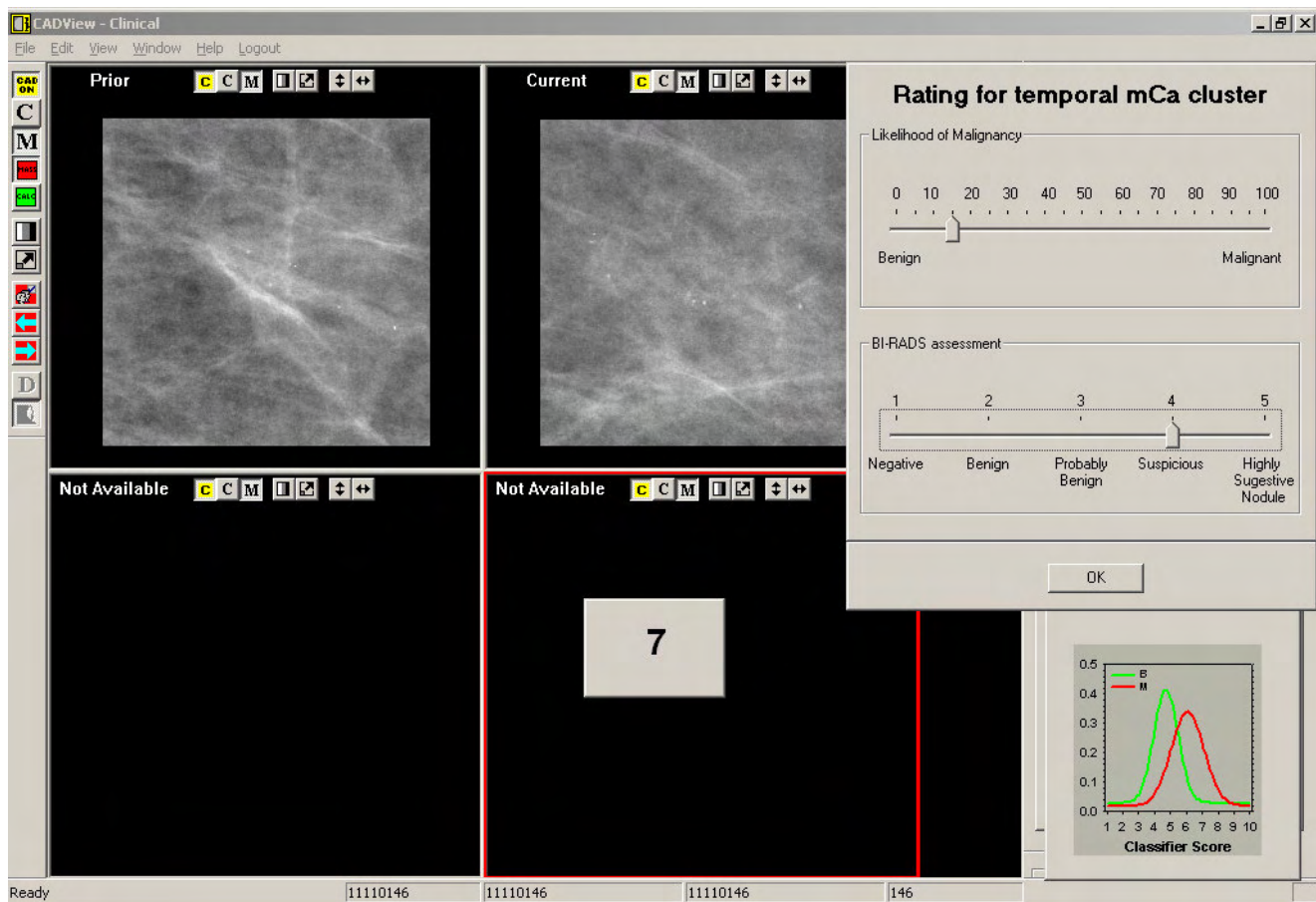


Figure 14. Graphical interface used in the observer study. The example shown was reading in the mode with computer aid. The image on the left is prior, the image on the right is current. The computer rating was shown in the lower middle part of the screen. The performance of the computer classifier in terms of the distribution of the relative malignancy rating was shown in the lower right corner. The radiologist first evaluated the mass without CAD (Figure 13) and could change the likelihood of malignancy and/or the BI-RADS assessment after taking into consideration the computer's rating.

Results

The CAD system alone achieved a test A_z of 0.82 for this data set. For the 8 radiologists, the average A_z in estimating the LM was 0.69 (range:0.63–0.73) without CAD and improved to 0.75 (range:0.68–0.82) with CAD (Figure 15). The improvement was statistically significant ($p=0.005$).

Similar trend can be observed for the partial area index $A_z^{(0.90)}$ for the reading without and with CAD (Figure 16). The improvement in the radiologists' classification accuracy with CAD ($A_z^{(0.90)}=0.15$ (range:0.06-0.27)) compared to the reading without CAD ($A_z^{(0.90)}=0.08$ (range:0.04-0.16)) was statistically significant ($p=0.03$).

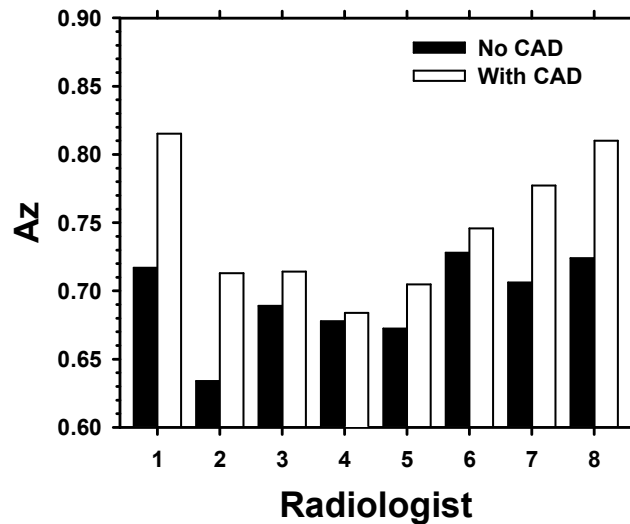


Figure 15. The area under ROC curve for the characterization of the microcalcification clusters without CAD and with CAD by the 8 radiologists. Average ROC results for the two reading modes: without CAD ($A_z=0.69$) and with CAD ($A_z=0.75$).

Based on BI-RADS assessments the radiologists with CAD would perform 5.6% (5.25/94) more biopsies for malignant masses on average and reduced 1.5% (1.5/167) unnecessary biopsies for benign masses.

The computer A_z value of 0.82 was higher than the individual radiologists' A_z values obtained in the independent mode without CAD. All 8 radiologists showed improvement when they used CAD. One radiologists achieved an A_z equal to that of the computer classifier in the reading with CAD. For the rest of the radiologists the improvement in A_z ranged between 0.01 and 0.1.

In this observer study the radiologists improved their performance with statistical significance when their reading without computer aid was compared to that with computer aid. These results suggest that CAD may be helpful in improving the accuracy of malignant and benign mass characterization.

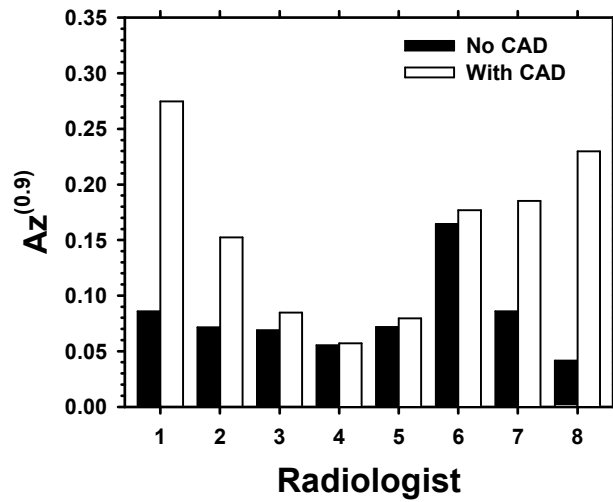


Figure 16. The partial area under ROC curve for the characterization of the microcalcification clusters without CAD and with CAD by the 8 radiologists. Average ROC results for the two reading modes: without CAD ($A_z^{(0.90)}=0.08$) and with CAD ($A_z^{(0.90)}=0.15$).

The results of this study were presented at RSNA2006 [A5], RSNA2006 [A6] and additionally will be presented at RSNA2007 [A7]. We also are preparing a manuscript which will be submitted to the journal of Radiology.

This observer study indicates that CAD using interval change analysis can significantly improve radiologists' accuracy in classification of clustered microcalcifications on serial mammograms and it may be useful for assisting radiologists in classification of masses and thereby reducing unnecessary biopsies and performing the correct biopsies on malignant clustered microcalcifications. This type of observer study is new and unique and the outcome is important, providing a new understanding of the potentials of computer aid to the radiologists in characterization of the temporal changes of mammographic microcalcification clusters.

(6) Key research accomplishments in current year as a result of this grant

- Collection of a temporal microcalcification database consisting of malignant and benign breast microcalcification cases that have multiple examinations (collection of temporal cases and extraction of regions of interest) (Task 1).
- Development and evaluation of regional registration techniques (RRM, AF, TPS) for localization of a search region for the corresponding microcalcification cluster on the prior mammogram of the same view (Task 2).
- Successfully adapt the automated detection method for improved identification of candidates of microcalcification clusters within the search region (Task 3).
- Development of feature extraction techniques and definition of different type similarity measures for matching corresponding microcalcification clusters on current and prior mammograms (Task 4).
- Design and evaluation of a correspondence classifier for identification of matched cluster pairs on current and prior mammograms and eliminate false pairs based on extracted features (Task 5).
- Development and evaluation of LDA, SVM and NN classifiers for classification on malignant and benign interval clusters based on automatically detected clusters and individual microcalcifications (Task 6).
- Comparison of temporal classifier and classifier based on current microcalcification clusters (Task 7).
- Performing an observer study with eight radiologists evaluating temporal pairs of microcalcification clusters without and with CAD (Task 8).

(7) Reportable Outcomes

7.1 Publications as a result of this grant

Conference proceedings

- [C1] Hadjiiski L, D Drouillard, HP Chan, B Sahiner, MA Helvie, MA Roubidoux, C Zhou, "Characterization of corresponding microcalcification clusters on temporal pairs of mammograms for interval change analysis: comparison of classifiers" *Proc. SPIE Medical Imaging*, 2006, 6144: 5Q1-5Q6.

Abstracts

- [A1] Hadjiiski L, HP Chan, B Sahiner, C Zhou, MA Helvie, MA Roubidoux, "Computerized Regional Registration of Corresponding Masses and Microcalcification Clusters on Temporal Pairs of Mammograms for Interval Change Analysis", *89th Scientific Assembly and Annual Meeting of the Radiological Society of North America (RSNA)*, Chicago, Illinois, 2003, pp. 389.

- [A2] Hadjiiski L, HP Chan, B Sahiner, MA Helvie, MA Roubidoux, C Zhou, "Interval change analysis based on computerized regional registration of corresponding microcalcification clusters on temporal pairs of mammograms," *90th Scientific Assembly and Annual Meeting of the Radiological Society of North America*, Chicago, IL, Nov. 28-Dec 3, 2004, pp. 491.
- [A3] Hadjiiski L, HP Chan, B Sahiner, MA Helvie, MA Roubidoux, C Zhou, "Interval change analysis of corresponding clustered microcalcifications on serial mammograms based on automated regional registration," *Era of Hope Meeting*, U. S. Army Medical Research and Materiel Command, Department of Defense, Breast Cancer Research Program, Philadelphia, PE, June 8-11, 2005, pp. 107.
- [A4] Hadjiiski L, HP Chan, B Sahiner, MA Helvie, MA Roubidoux, C Zhou, "Automated regional registration and classification of corresponding microcalcification clusters on serial mammograms," *91th Scientific Assembly and Annual Meeting of the Radiological Society of North America*, Chicago, IL, Nov. 27-Dec 2, 2005, pp. 270.
- [A5] Hadjiiski L, HP Chan, B Sahiner, MA Roubidoux, MA Helvie, CParamagul, AV Nees, J Bailey, SK Patterson, "ROC Study: Effects of Computer-Aided Diagnosis on Radiologists' Characterization of Malignant and Benign Breast Clustered Microcalcifications in Temporal Pairs of Mammograms," *92nd Scientific Assembly and Annual Meeting of the Radiological Society of North America*, Chicago, IL. Nov. 26 – Dec. 1, 2006, pp. 284.
- [A6] Hadjiiski L, HP Chan, B Sahiner, AV Nees, J Bailey, SK Patterson, MA Roubidoux, MA Helvie, C Paramagul, "Computer-Aided Characterization of Malignant and Benign Breast Clustered Microcalcifications on Serial Mammograms: Early Experience of its Effects on Radiologists' Performance from an ROC Study," *92nd Scientific Assembly and Annual Meeting of the Radiological Society of North America*, Chicago, IL. Nov. 26 – Dec. 1, 2006, pp. 933.
- [A7] Hadjiiski L, P Filev, HP Chan, B Sahiner, MA Roubidoux, MA Helvie, C Paramagul, AV Nees, SK Patterson, C Blane, R Pinsky, A Joe, J Bailey, "ROC Study: Computer-Aided Diagnosis of Malignant and Benign Breast Clustered Microcalcifications in Temporal Pairs of Mammograms and its Effect on Radiologists' Characterization Performance", Accepted for presentation at the *93rd Scientific Assembly and Annual Meeting of the Radiological Society of North America*, Chicago, IL, November 25-30, 2007.

Presentations

- [P1] Hadjiiski L, HP Chan, B Sahiner, C Zhou, MA Helvie, MA Roubidoux, "Computerized Regional Registration of Corresponding Masses and Microcalcification Clusters on Temporal Pairs of Mammograms for Interval Change Analysis", Presented at the *89th Scientific Assembly and Annual Meeting of the Radiological Society of North America (RSNA)*, Chicago, Illinois, 2003.
- [P2] Hadjiiski L, HP Chan, B Sahiner, MA Helvie, MA Roubidoux, C Zhou, "Interval change

- analysis based on computerized regional registration of corresponding microcalcification clusters on temporal pairs of mammograms,” Presented at the *90th Scientific Assembly and Annual Meeting of the Radiological Society of North America*, Chicago, IL, Nov. 28-Dec 3, 2004.
- [P3] Hadjiiski L, HP Chan, B Sahiner, MA Helvie, MA Roubidoux, C Zhou, “Interval change analysis of corresponding clustered microcalcifications on serial mammograms based on automated regional registration,” **Oral Presentation** at the *Era of Hope Meeting*, U. S. Army Medical Research and Materiel Command, Department of Defense, Breast Cancer Research Program, Philadelphia, PE, June 8-11, 2005.
- [P4] Hadjiiski L, HP Chan, B Sahiner, MA Helvie, MA Roubidoux, C Zhou, “Interval change analysis of corresponding clustered microcalcifications on serial mammograms based on automated regional registration,” **Poster Presentation** at the *Era of Hope Meeting*, U. S. Army Medical Research and Materiel Command, Department of Defense, Breast Cancer Research Program, Philadelphia, PE, June 8-11, 2005.
- [P5] Hadjiiski L, HP Chan, B Sahiner, MA Helvie, MA Roubidoux, C Zhou, “Automated regional registration and classification of corresponding microcalcification clusters on serial mammograms,” Presented at the *91th Scientific Assembly and Annual Meeting of the Radiological Society of North America*, Chicago, IL, Nov. 27-Dec 2, 2005.
- [P6] Hadjiiski L, D Drouillard, HP Chan, B Sahiner, MA Helvie, MA Roubidoux, C Zhou, “Characterization of corresponding microcalcification clusters on temporal pairs of mammograms for interval change analysis: comparison of classifiers” Presented at *SPIE Medical Imaging*, San Diego, CA, Feb 11- Feb 16, 2006.
- [P7] Hadjiiski L, HP Chan, B Sahiner, MA Roubidoux, MA Helvie, CParamagul, AV Nees, J Bailey, SK Patterson, “ROC Study: Effects of Computer-Aided Diagnosis on Radiologists’ Characterization of Malignant and Benign Breast Clustered Microcalcifications in Temporal Pairs of Mammograms,” Presented at the *92nd Scientific Assembly and Annual Meeting of the Radiological Society of North America*, Chicago, IL. Nov. 26 – Dec. 1, 2006.
- [P8] Hadjiiski L, HP Chan, B Sahiner, AV Nees, J Bailey, SK Patterson, MA Roubidoux, MA Helvie, C Paramagul, “Computer-Aided Characterization of Malignant and Benign Breast Clustered Microcalcifications on Serial Mammograms: Early Experience of its Effects on Radiologists’ Performance from an ROC Study,” Education exhibit, *92nd Scientific Assembly and Annual Meeting of the Radiological Society of North America*, Chicago, IL. Nov. 26 – Dec. 1, 2006.
- [P9] Hadjiiski L, P Filev, HP Chan, B Sahiner, MA Roubidoux, MA Helvie, C Paramagul, AV Nees, SK Patterson, C Blane, R Pinsky, A Joe, J Bailey, “ROC Study: Computer-Aided Diagnosis of Malignant and Benign Breast Clustered Microcalcifications in Temporal Pairs of Mammograms and its Effect on Radiologists’ Characterization Performance”, To be presented at the *93rd Scientific Assembly and Annual Meeting of the Radiological Society of North America*, Chicago, IL, November 25-30, 2007.

Copies of publications are enclosed with this report.

7.2 Awards as a result of this grant

- [1] “Certificate of Merit”, Radiological Society of North America, Nov. 2006, Authors: Hadjiiski L, Chan HP, Sahiner B, Nees AV, Bailey JE, Patterson SK, *et al.*, In recognition of excellence of the Education Exhibit “Computer-Aided Characterization of Malignant and Benign Breast Clustered Microcalcifications on Serial Mammograms: Early Experience of its Effects on Radiologists’ Performance from an ROC Study,” Education exhibit, *92nd Scientific Assembly and Annual Meeting of the Radiological Society of North America*, Chicago, IL. Nov. 26 – Dec. 1, 2006.

Copy of the award certificate is enclosed with this report.

7.3 Personnel participating in the research effort as a result of this grant

Lubomir Hadjiiski, Ph.D.	–	P.I.
Mark Helvie, M.D.	–	Co-Investigator
Marilyn Robidoux, M.D.	-	Co-Investigator
Heang-Ping Chan, Ph.D.	-	Consultant
Charles Meyer, Ph.D.	-	Consultant
Peter Filev, BS	-	Research Technician Associate
Momchil Filev	-	Research Assistant
Ethan Sreet	-	Research Assistant
Douglas Drouillard	-	Research Assistant
Daniel Schuster	-	Research Assistant

(8) Conclusion

As a result of the support by the USAMRMC grant, we have (1) collected a data set of cases with temporal microcalcification clusters; (2) Applied the RRM for the localization of the search region for the corresponding microcalcification cluster on the prior mammogram; (3) Adapted the automated detection method for identification of candidates of microcalcification clusters within the search region; (4) Extracted texture and morphological features and defined difference similarity measures for matching corresponding microcalcification clusters on current and prior mammograms from automatically detected microcalcification clusters; (5) Design a correspondence classifier for identification of matched cluster based on extracted features and the difference similarity measures; (6) Develop feature measures and LDA, NN, and SVM temporal classifiers for characterization of temporal changes in automatically detected microcalcification clusters; (7) Compare the temporal classifier with classifier based on current images only; (8) Perform an observer study.

The obtained results showed the feasibility of the proposed approach. The RRM allowed to have all the clusters within the search region on the prior mammogram. We were successful to adapt and improve the automated microcalcification detection system to be more sensitive for identification of candidates of microcalcification clusters within the local search region. It was able to detect substantially more true clusters without increasing the FP rate compared to the conventional detection system. The squared difference similarity measure applied to the enhanced morphological features was the successful combination for the input to the correspondence classifier. The correspondence classifier was able to reduce the TP-FP pairs resulting in less FP clusters within the search region on prior. The new classification scheme, using interval change information, was able successfully to classify mammographic microcalcification clusters as malignant and benign and it was performing better than the classifier based on current images only. Morphological ratio features, difference RLS features and current GLDS features were useful for the classification.

We were able to design a CAD system for automatic characterization of temporal cases on malignant and benign. The radiologist initially points to the microcalcification cluster of interest on the current mammogram and then the CAD system can automatically allocate the corresponding region on the prior mammogram and perform malignant/benign classification based both on the current and prior information. The design of an automatic CAD is challenging. The automatically detected cluster locations on the temporal pairs may deviate from the optimal locations as selected by expert radiologists. This will introduce “noise” to the extracted features and make the classification task more difficult. We were able to overcome the above difficulties related to for the design of an automatic CAD. A feature extraction and classification was carried out with the clusters and individual microcalcifications obtained automatically from the registration stage. Based on these features we have designed a classification scheme to classify the automatically registered and detected microcalcification clusters. This temporal classifier performed better than the classifier based on current images only.

We performed an observer study for evaluation of the radiologist performance without and with CAD. Eight radiologists participated in the study. The radiologists improved their performance when using CAD. The improvement was statistically significant. This observer study indicates that CAD using interval change analysis can significantly improve radiologists’ accuracy in classification of clustered microcalcifications on serial mammograms and it may be useful for assisting radiologists in classification of masses and thereby reducing unnecessary biopsies and

performing the correct biopsies on malignant clustered microcalcifications. CAD using interval change analysis may increase the positive predictive value of mammography.

(9) References

1. Petrick N, Chan HP, Wei D, Sahiner B, Helvie MA and Adler DD, "Automated detection of breast masses on mammograms using adaptive contrast enhancement and texture classification," *Med Phys* 23, 1685-1696 (1996).
2. Zhou C, Chan H, Petrick N, Helvie M, Goodsitt M, Sahiner B and Hadjiiski L, "Computerized image analysis: Estimation of breast density on mammograms.," *Med Phys*, 28 (6), 1056-1069, (2001).
3. Zhou C, HP Chan, C Paramagul, MA Roubidoux, B Sahiner, LM Hadjiiski, N Petrick, "Computer-aided diagnosis on mammograms using multiple image analysis: computerized nipple identification," *Med Phys*, 31, 2871-2882 (2004).
4. S.S. Gopal, H.P. Chan, T.E. Wilson, M.A. Helvie, N. Petrick, B. Sahiner, "A regional registration technique for automated interval change analysis of breast lesions on mammograms", *Med Phys*, 1999, 26, 2669-2679.
5. L. Hadjiiski, H.P. Chan, B. Sahiner, N. Petrick, M. Helvie, "Automated Registration of Breast Lesions in Temporal Pairs of Mammograms for Interval Change Analysis – Local Affine Transformation for Improved Localization", *Med Phys*, 28 (6), June 2001, pp. 1070-1079.
6. Rao SS, *Optimization: Theory and Applications*, (Wiley Eastern Limited, 1979).
7. Lootsma FA, *Numerical methods for non-linear optimization*, (Academic Press, New York, 1972).
8. Quan L and Kanade T, "Affine structure from line correspondance with uncalibrated affine cameras," *IEEE Trans Pat Anal Machine Intel* 19, 834-845 (1997).
9. Bookstein LF, *Morphometric Tools for Landmark Data*, (Cambridge University Press, Cambridge, 1991).
10. Bookstein FL and Green WDKA, "A feature spase for edgels in images with landmarks," *J Math Imag Vision* 3, 231-261 (1993).
11. Meyer CR, Boes JL, Kim B, Bland P, Zasadny KR, Kison PC, Koral K, Frey KA and Wahl RL, "Demonstration of accuracy and clinical versatility of mutual information for automatic multimodality image fusion using affine and thin plate spline warped geometric deformations," *Medical Image Analysis* 3, 195-206 (1997).
12. Chan HP, Lo SCB, Sahiner B, Lam KL and Helvie MA, "Computer-aided detection of mammographic microcalcifications: Pattern recognition with an artificial neural network," *Med Phys* 22, 1555-1567 (1995).
13. Haralick RM, Shanmugam K and Dinstein I, "Texture features for image classification," *IEEE Trans Sys Man and Cybern SMC-3*, 610-621 (1973).
14. Sahiner B, Chan HP, Petrick N, Wei D, Helvie MA, Adler DD and Goodsitt MM, "Classification of mass and normal breast tissue: A convolution neural network classifier with spatial domain and texture images," *IEEE Trans Med Img* 15, 598-610 (1996).
15. Weszka JS, Dyer CR and Rosenfeld A, "A comparative study of texture measures for terrain classification," *IEEE Trans Sys Man and Cybern* 6, 269-285 (1976).
16. Filev P, L Hadjiiski, B Sahiner, H-P Chan, MA Helvie, "Comparison of similarity measures for the task of template matching of masses on serial mammograms," *Med Phys* 2005, 32 (2), 515-529.
17. Hadjiiski L, B Sahiner, HP Chan, N Petrick, MA Helvie "Automated interval change analysis

- of masses in serial mammograms - evaluation of an adaptive similarity measure for mass matching,” *Proc. Digital Mammography IWDM 2004: 7th International Workshop on Digital Mammography* (Ed. Pisano E. 534-539).
18. L. Hadjiiski, H.P. Chan, M. Gurcan, B. Sahiner, N. Petrick, M.A. Helvie, M. Roubidoux “Computer-Aided Characterization of Malignant and Benign Microcalcification Clusters Based on the Analysis of Temporal Change of Mammographic Features”, Presented at the *SPIE International Symposium on Medical Imaging*, San Diego, California, February 23-28, 2002. *Proc. SPIE Medical Imaging, 2002, 4684, pp.749-753*.
 19. V. N. Vapnik, *Statistical Learning Theory*, Wiley, New York, 1998.
 20. Dorfman, D.D., K.S. Berbaum, and C.E. Metz, *ROC rating analysis: Generalization to the population of readers and cases with the jackknife method*. *Invest. Radiol.*, 1992. **27**: p. 723-731.

(10) Appendix

Copies of publications are enclosed with this report.

Characterization of Corresponding Microcalcification Clusters on Temporal Pairs of Mammograms for Interval Change Analysis - Comparison of Classifiers

Lubomir Hadjiiski*, Douglas Drouillard, Heang-Ping Chan, Berkman Sahiner, Mark A. Helvie, Marilyn Roubidoux, Chuan Zhou

Department of Radiology, University of Michigan, Ann Arbor, MI 48109

ABSTRACT

We are developing an automated system for analysis of microcalcification clusters on serial mammograms. Our automated system consists of two stages: (1) automatic registration of corresponding clusters on temporal pairs of mammograms producing true (TP-TP) and false (TP-FP) pairs; and (2) characterization of temporal pairs of clusters as malignant and benign using a temporal classifier. In this study, we focussed on the design of the temporal classifier. Morphological and texture (RLS and GLDS) features are automatically extracted from the detected current and prior cluster locations. Additionally, difference morphological and RLS features are obtained. The automatically detected cluster locations on the temporal pairs may deviate from the optimal locations as selected by expert radiologists. This will introduce “noise” to the extracted features and make the classification task more difficult. Linear discriminant analysis (LDA) and support vector machine (SVM) classifiers were trained to classify the true and false pairs. Leave-one-case-out resampling method was used for feature selection and classifier design. In this study, 175 serial mammogram pairs containing biopsy-proven microcalcification clusters were used. At the first stage of the system, 85% (149/175) of the TP-TP pairs were identified with 15 false matches within the 164 image pairs that had computer-detected clusters on the priors. At the second stage, an average of 7 features were selected (4 difference morphological, 1 difference RLS and 2 current GLDS). The LDA and SVM temporal classifiers achieved test A_z of 0.83 and 0.82, respectively, for the classification of the 164 cluster temporal pairs as malignant or benign. In comparison, an MQSA radiologist achieved an A_z of 0.72. Both the LDA and SVM classifiers were able to classify the automatically detected temporal pairs of microcalcification clusters with accuracy comparable to that of an experienced radiologist.

Keywords: Computer-Aided Diagnosis, Interval Changes, Microcalcification Classification, Feature analysis, Mammography, Malignancy.

1. INTRODUCTION

Mammography is currently the most effective method for early breast cancer detection^{1,2}. Radiologists routinely compare mammograms from a current examination with those obtained in previous years, if available, for identifying interval changes, detecting potential abnormalities, and evaluating breast lesions. It is widely accepted that analysis of interval changes in mammographic features is very useful for both detection and classification of abnormalities^{3,4}. A variety of computer-aided diagnosis (CAD) techniques have been developed to detect mammographic abnormalities and to distinguish between malignant and benign lesions. We are studying the use of CAD techniques to assist radiologists in interval change analysis.

Commonly used classification methods for CAD use information from a single examination. These methods have been shown to perform well in lesion classification problems⁵⁻¹⁴. However, when multiple-year mammograms of a

* L. H. (correspondence): e-mail: lhadjiski@umich.edu

lesion are available, it is not trivial to design computer vision methods to use the temporal information for computer-aided classification and to improve the differentiation between benign and malignant masses.

The goal of our research is to develop a technique for computerized analysis of temporal differences between a microcalcification cluster on the most recent mammogram and a prior mammogram of the same view¹⁵. The computer system can be used to assist radiologists in evaluating interval changes and thus distinguishing between malignant and benign microcalcification clusters for CAD. It will also be useful for improving the identification of new or growing clusters in a detection system or for improved classification of malignant and benign clusters in a diagnostic system. In our previous studies we have demonstrated that interval change analysis can improve differentiation of malignant and benign masses^{16,17}.

The purpose of this study is to compare the performance of different classifiers for the task of automated characterization of microcalcification clusters using interval change information on serial mammograms. With an automated system, noise is introduced by the imperfect registration and imperfect detection of the clusters on both current and prior mammograms. This analysis will be useful for understanding the advantages and limitations of the classifiers when performing in noisy conditions.

2. MATERIALS AND METHODS

Our automated system consists of two stages: (1) registration of corresponding clusters on temporal pairs of mammograms, and (2) characterization of the temporal pairs of clusters as malignant and benign (Fig. 1). A description of the detection method and the database used is given below.

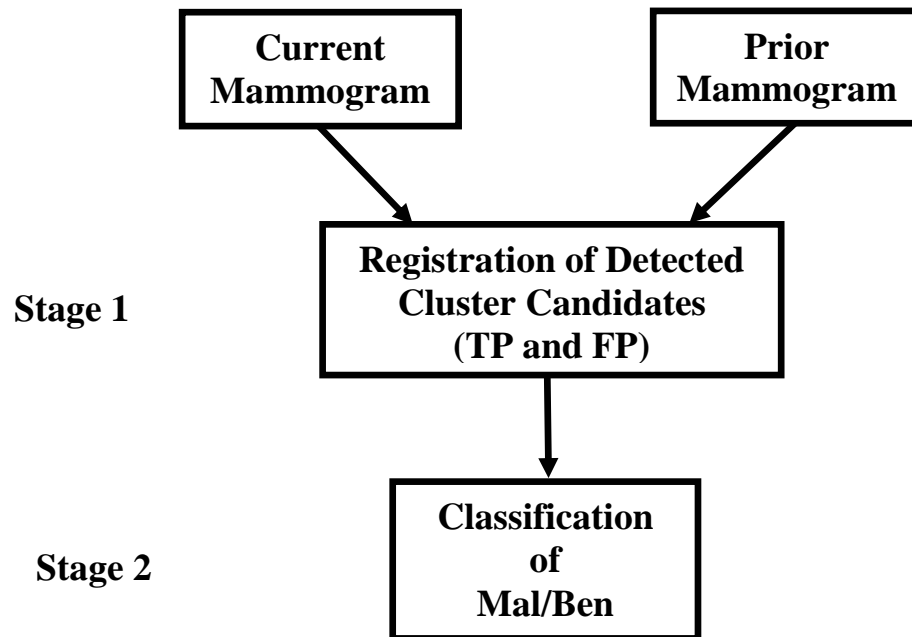


Figure 1. Block-diagram of the registration – classification CAD for temporal microcalcification clusters.

2.1 Registration of corresponding microcalcification clusters in serial mammograms

In the first stage, based on the location of a detected cluster on the current mammogram, a regional registration procedure identifies the local area on the prior that may contain the corresponding cluster. An automated detection program is used to detect cluster candidates within the local area (Fig. 2) that may include true positives (TP) and false positives (FPs). The cluster on the current image is then paired with the candidates to form true (TP-TP) or false (TP-FP) pairs (Fig. 2). A correspondence classifier is used to reduce the false pairs (TP-FP). This technique was presented in detail previously¹⁸.

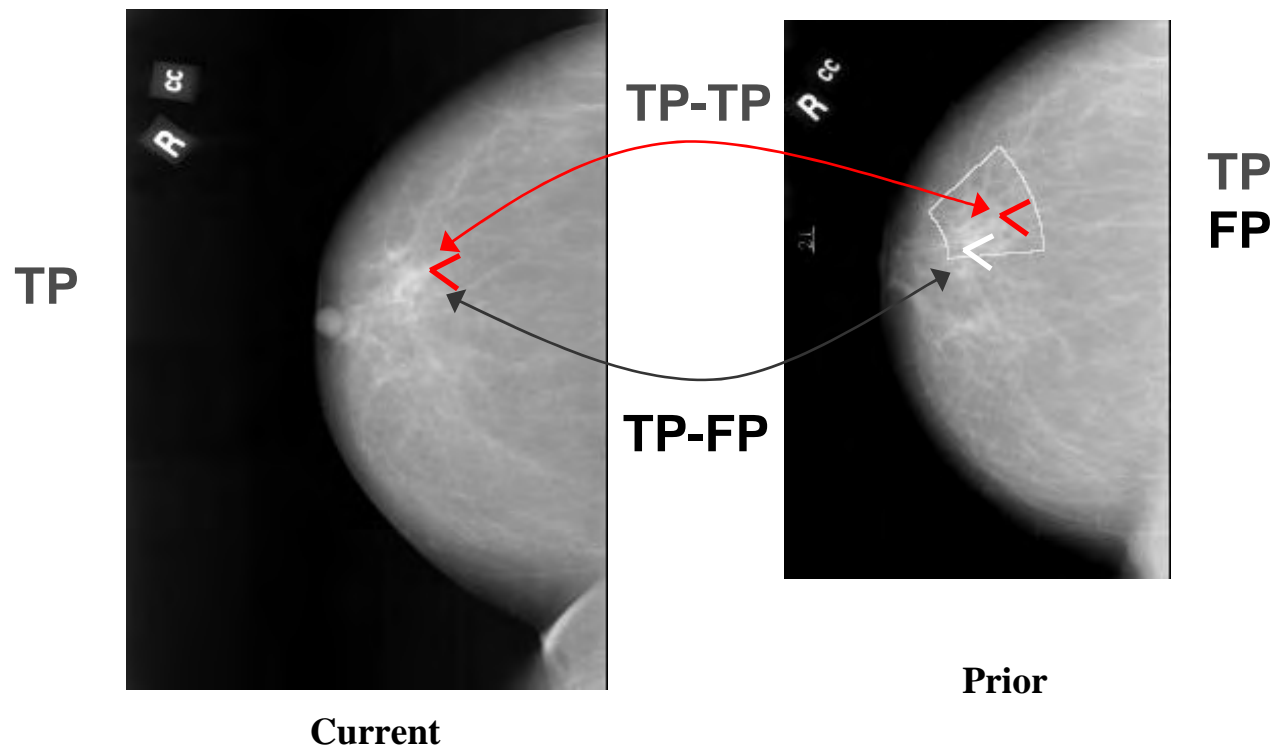


Figure 2. Automated registration resulting in true (TP-TP) and false (TP-FP) pairs by pairing the cluster on the current image with the detected TP and FP candidates on prior image.

2.2 Classification of automatically detected and registered temporal pairs of microcalcification clusters

In the second stage, a temporal classifier based on current and prior information is used if a cluster is detected on the prior, and a current classifier based on current information alone is used if no prior cluster is detected. In this study, we focussed on the design of the temporal classifier (Fig. 3). Morphological and texture features including run length statistics (RLS) and gray level dependance statistics (GLDS) are automatically extracted from the detected current and prior cluster locations. Sixty four GLDS features, 20 morphological features and 20 RLS features and the cluster size were extracted. Additionally, 20 difference morphological and 20 difference RLS features are obtained by subtracting a prior feature from the corresponding current feature. The automatically detected cluster locations on the temporal pairs may deviate from the optimal locations as selected by expert radiologists. This will introduce “noise” to the extracted features and make the classification task more difficult. Linear discriminant analysis (LDA) and support vector machine¹⁹ (SVM) classifiers were trained to classify the true and false pairs.

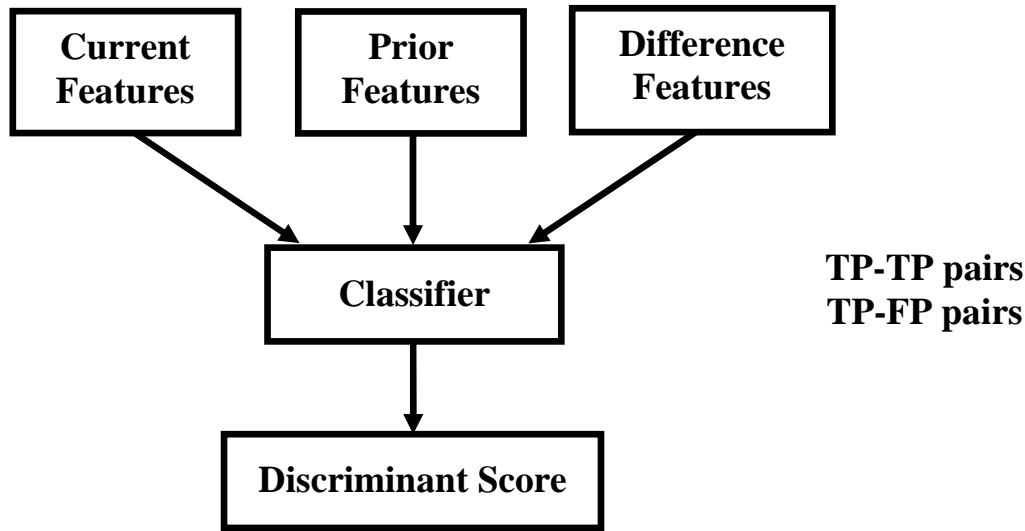


Figure 3. Block-diagram of the temporal classifier for classification of malignant and benign microcalcification clusters. Both TP-TP and TP-FP pairs can be input to the system.

2.3 Data set

In this study, 175 serial mammogram pairs containing biopsy-proven microcalcification clusters were used, of which 51 were biopsy-proven to be malignant and 124 benign. An experienced MQSA radiologist identified the gold standard cluster locations on corresponding mammogram pairs. On the priors, the radiologist rated 12 of the 175 clusters as not visible and the subtlety of 18 clusters as 9 or 10 on a scale of 10 (1=most obvious, 10=subtlest).

The mammograms were digitized with a LUMISCAN 85 laser scanner at a pixel resolution of $50\mu m \times 50\mu m$ and 4096 gray levels. The image matrix size was reduced by averaging every 2×2 adjacent pixels and down-sampled by a factor of 2 to obtain images with a pixel size of $100\mu m \times 100\mu m$ for analysis by the computer.

2.4 ROC analysis

Leave-one-case-out resampling method was used for feature selection and classifier design. Stepwise feature selection was used to obtain the best feature set. To evaluate the classifier performance, the training and test discriminant scores were analyzed using receiver operating characteristic (ROC) methodology²⁰. The discriminant scores of the malignant and benign microcalcification clusters were used as decision variables in the LABROC1 program²¹, which fits a binormal ROC curve based on maximum likelihood estimation. The classification accuracy was evaluated as the area under the ROC curve, A_z .

3. RESULTS

At the first stage of the system, 85% (149/175) of the TP-TP pairs were identified with 15 false matches within the 164 image pairs that had computer detected clusters on the priors. Therefore 164 temporal image pairs (149 TP-TP and 15 TP-FP), of which 49 were malignant, were used for classification as malignant and benign. At the second stage, an average of 7 features were selected. The selected features included 4 difference morphological features, 1 difference RLS feature and 2 GLDS features from the current image. The SVM and LDA temporal classifiers were used for the classification of the 164 cluster temporal pairs. SVMs with dot kernel, radial kernel and tanh kernel (neural kernel) were

studied. The training and testing results are presented in Table 1. The SVM classifier achieved test A_z of 0.82 ± 0.03 . The LDA classifier achieved test A_z of 0.83 ± 0.03 . In comparison, the MQSA radiologist achieved an A_z of 0.72 ± 0.04 for the 164 temporal pairs. The difference in A_z between any one of the classifiers and the radiologist did not achieve statistical significance.

Table 1. SVM classification results based on 7 selected features.

SVM Type	Training A_z	Test A_z	Number SV
Dot Kernel	0.87 ± 0.03	0.82 ± 0.03	78
Radial Kernel	0.86 ± 0.03	0.81 ± 0.03	89
Tanh Kernel	0.86 ± 0.03	0.82 ± 0.03	83

4. CONCLUSION

We studied the use of the LDA and SVM classifiers for the classification of automatically detected temporal pairs of microcalcification clusters as malignant or benign. Both the LDA and SVM classifiers were able to classify the automatically detected temporal pairs of microcalcification clusters with an accuracy comparable to that of an experienced radiologist. The SVMs with dot kernel, radial kernel, and tanh kernel had comparable performance with the radial kernel being slightly worse than the other two. The LDA and SVM classifiers also had comparable performance.

ACKNOWLEDGMENTS

This work was supported by USAMRMC grants DAMD17-02-1-0489. The authors are grateful to Charles E. Metz, Ph.D., for the LABROC program.

REFERENCES

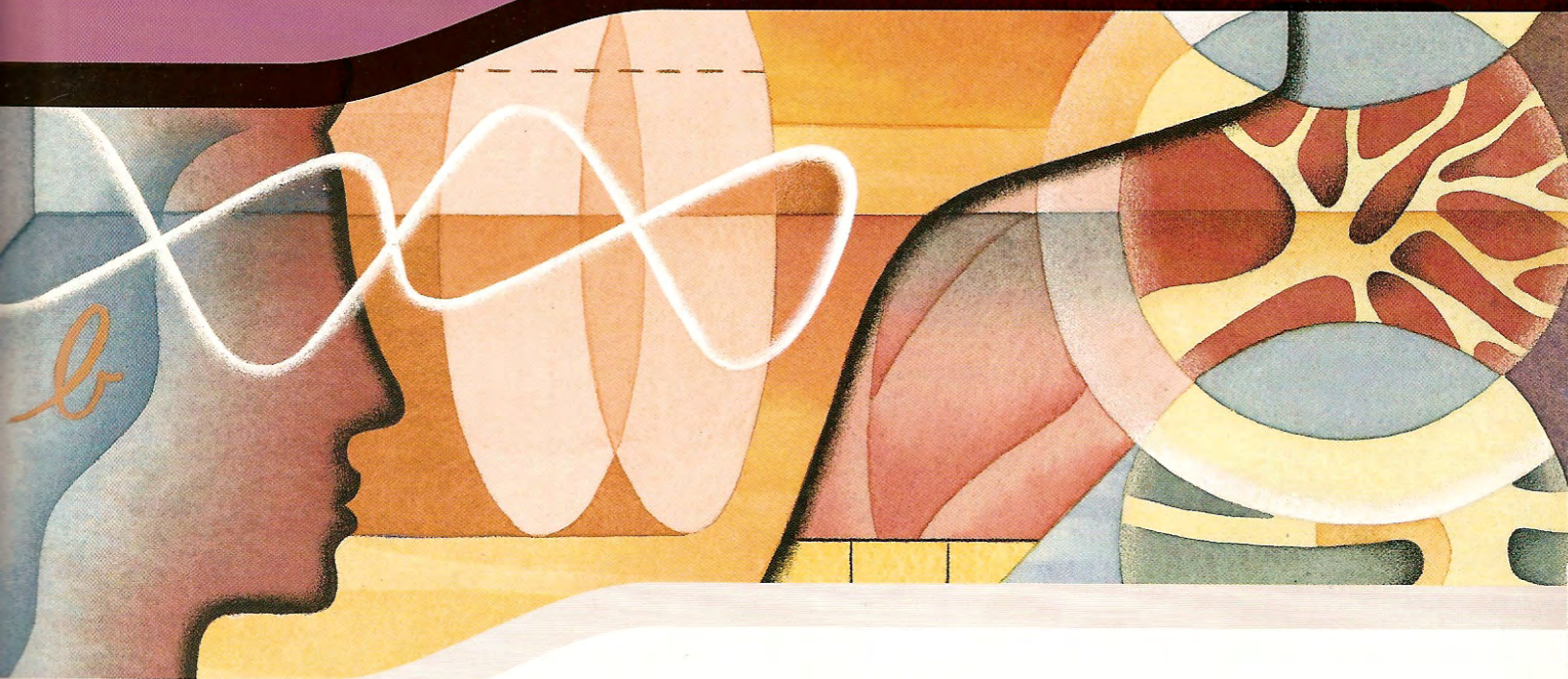
1. S. A. Feig, C. J. D'Orsi, R. E. Hendrick, V. P. Jackson, D. B. Kopans, B. Monsees, E. A. Sickles, C. B. Stelling, M. Zininger, and P. Wilcox-Buchalla, "American College of Radiology guidelines for breast cancer screening," *AJR Am J Roentgenol.* **171**, 29-33, 1998.
2. B. Cady and J. S. Michaelson, "The life-sparing potential of mammographic screening," *CANCER* **91**, 1699-1703, 2001.
3. L. W. Bassett, B. Shayestehfar, and I. Hirbawi, "Obtaining previous mammograms for comparison: usefulness and costs," *American Journal of Roentgenology* **163**, 1083-1086, 1994.
4. E. S. Burnside, E. A. Sickles, R. E. Sohlich, and K. E. Dee, "Differential Value of Comparison with Previous Examinations in Diagnostic Versus Screening Mammography," *Amer. J. Roentgenology* **179**, 1173-1177, 2002.
5. H. P. Chan, D. Wei, K. L. Lam, B. Sahiner, M. A. Helvie, D. D. Adler, and M. M. Goodsitt, "Classification of malignant and benign microcalcifications by texture analysis," *Medical Physics* **22**, 938, 1995.
6. Y. Jiang, R. M. Nishikawa, D. E. Wolverton, C. E. Metz, M. L. Giger, R. A. Schmidt, C. J. Vyborny, and K. Doi, "Malignant and benign clustered microcalcifications: automated feature analysis and classification," *Radiology* **198**, 671-678, 1996.

7. H. P. Chan, B. Sahiner, N. Petrick, M. A. Helvie, K. L. Leung, D. D. Adler, and M. M. Goodsitt, "Computerized classification of malignant and benign microcalcifications on mammograms: texture analysis using an artificial neural network," *Physics in Medicine and Biology* **42**, 549-567, 1997.
8. H. P. Chan, B. Sahiner, K. L. Lam, N. Petrick, M. A. Helvie, M. M. Goodsitt, and D. D. Adler, "Computerized analysis of mammographic microcalcifications in morphological and texture feature space," *Medical Physics* **25**, 2007-2019, 1998.
9. Y. Jiang, R. M. Nishikawa, and J. Papaioannou, "Dependence of computer classification of clustered microcalcifications on the correct detection of microcalcifications " *Medical Physics* **28**, 1949-1957, 2001.
10. M. F. Salfity, R. M. Nishikawa, Y. Jiang, and J. Papaioannou, "The use of a priori information in the detection of mammographic microcalcifications to improve their classification," *Medical Physics* **30**, 823-831, 2003.
11. S. Paquerault, L. M. Yarusso, J. Papaioannou, Y. Jiang, and R. M. Nishikawa, "Radial gradient-based segmentation of mammographic microcalcifications: Observer evaluation and effect on CAD performance," *Medical Physics* **31**, 2648-2657, 2004.
12. M. Kallergi, "Computer-aided diagnosis of mammographic microcalcification clusters," *Medical Physics* **31**, 314-326, 2004.
13. I. Leichter, R. Lederman, S. S. Buchbinder, P. Bamberger, B. Novak, and S. Fields, "Computerized Evaluation of Mammographic Lesions: What Diagnostic Role Does the Shape of the Individual Microcalcifications Play Compared with the Geometry of the Cluster?," *AJR Am J Roentgenol.* **2004**, 705-712, 2004.
14. L. Wei, Y. Yang, R. M. Nishikawa, and Y. Jiang, "A Study on Several Machine-Learning Methods for Classification of Malignant and Benign Clustered Microcalcifications," *IEEE Trans Medical Imaging* **24**, 371-380, 2005.
15. L. M. Hadjiiski, H. P. Chan, B. Sahiner, N. Petrick, M. A. Helvie, M. A. Roubidoux, and M. N. Gurcan, "Computer-aided characterization of malignant and benign microcalcification clusters based on the analysis of temporal change of mammographic features," *Proc SPIE* **4684**, 749-753, 2002.
16. L. M. Hadjiiski, B. Sahiner, H. P. Chan, N. Petrick, M. A. Helvie, and M. N. Gurcan, "Analysis of Temporal Change of Mammographic Features: Computer-Aided Classification of Malignant and Benign Breast Masses," *Medical Physics* **28**, 2309-2317, 2001.
17. L. M. Hadjiiski, H. P. Chan, B. Sahiner, M. A. Helvie, M. Roubidoux, C. Blane, C. Paramagul, N. Petrick, J. Bailey, K. Klein, et al., "Improvement of Radiologists' Characterization of Malignant and Benign Breast Masses in Serial Mammograms by Computer-Aided Diagnosis: An ROC Study," *Radiology* **233**, 255-265, 2004.
18. L. M. Hadjiiski, H. P. Chan, B. Sahiner, M. A. Helvie, M. A. Roubidoux, and C. Zhou, "Interval Change Analysis Based on Computerized Regional Registration of Corresponding Microcalcification Clusters on Temporal Pairs of Mammograms," 491-491, RSNA Program Book 2004, 2004.
19. V. N. Vapnik, *Statistical Learning Theory*, Wiley, New York, 1998.
20. C. E. Metz, "ROC methodology in radiologic imaging," *Investigative Radiology* **21**, 720-733, 1986.
21. C. E. Metz, J. H. Shen, and B. A. Herman, "New methods for estimating a binormal ROC curve from continuously-distributed test results," *Annual Meeting of the American Statistical Association*, Anaheim, CA, 1990.



RSNA'03

COMMUNICATION FOR
BETTER PATIENT CARE



Radiological Society of North America **Scientific Assembly and Annual Meeting Program**

The Radiological Society of North America • 89th Scientific Assembly and Annual Meeting
November 30 – December 5, 2003 • McCormick Place, Chicago

RSNA® Radiological Society
of North America
Founded in 1915



American Association
of Physicists in Medicine

377 • 11:10 AM

Computerized Detection of Microcalcifications on Mammograms: Improved Detection Accuracy by Combining Features Extracted from Two Mammographic Views

B. Sahiner, PhD, Ann Arbor, MI • H. Chan, PhD • L.M. Hadjiiski, PhD • M.A. Helvie, MD • M.A. Roubidoux, MD • N.A. Petrick, PhD (berki@umich.edu)

PURPOSE: Analysis of the correspondence of the locations and features of lesion candidates on two mammographic views is a promising method for improving computerized lesion detection. In this study, we investigated the use of joint CC and MLO view information for detection of microcalcification clusters on mammograms, and compared the accuracy of this two-view detection method to our single-view detection method.

METHOD AND MATERIALS: Candidates of microcalcification clusters were located using our previously developed prescreening algorithm. In single-view detection, false-positives (FPs) among these candidates were reduced by using a classifier based on features extracted by a neural network, as well as the morphological and texture features extracted from the cluster. For two-view detection, object pairs from the CC and MLO view candidates were formed by using their radial distances from the nipple. The pairs were classified using a correspondence classifier, which analyzed the similarity between features in a pair. The correspondence classifier scored each pair as to its likelihood of being a true positive pair. These scores were fused with the single-view detection scores. The algorithm was trained using 108 mammogram pairs from our institution, and tested using an independent public data set from the University of South Florida (USF). The test set included 232 mammograms (116 two-view cases) containing 254 microcalcification clusters. Nine of the microcalcifications were seen only on one view. The FP rate was measured by applying the algorithm to 152 normal mammograms (76 two-view cases) from the USF database.

RESULTS: The prescreening algorithm detected 89% (226/254) of the clusters with an average of 3.5 FPs/image (539/152) on the normal mammograms. After FP reduction, the single-view detection algorithm had a film-based sensitivity of 86% at 0.6 FPs/image. At the same sensitivity, the two-view detection algorithm produced 0.4 FPs/image. The sensitivity of the single-view and two-view detection algorithms was 79% and 83%, respectively, at 0.1 FPs/image. If correct detection was defined as marking a malignant cluster on at least one view, the two-view detection algorithm achieved a sensitivity of 90% at 0.1 FPs/image.

CONCLUSIONS: The correspondence of geometric, morphological, textural and neural network features of cluster candidates on two different views provides valuable information for improving the accuracy of computerized microcalcification detection.

378 • 11:20 AM

Computerized Regional Registration of Corresponding Masses and Microcalcification Clusters on Temporal Pairs of Mammograms for Interval Change Analysis

L.M. Hadjiiski, PhD, Ann Arbor, MI • H. Chan, PhD • B. Sahiner, PhD • C. Zhou, PhD • M.A. Helvie, MD • M.A. Roubidoux, MD (lhadjisk@umich.edu)

PURPOSE: To develop a registration technique for automated identification of corresponding lesions on a temporal pair of mammograms of the same view. This technique is the basis for interval change analysis of breast lesions in CAD applications.

METHOD AND MATERIALS: A multi-stage registration technique is being developed. In the first stage, an initial search region was estimated on the prior mammogram based on the lesion location on the current mammogram. In the second stage the search region was refined. In the third stage the lesion was detected within the search region. For the initial estimation of the lesion centroid location on the prior mammogram, we previously developed a regional registration method (RRM), based on the radial distance between the nipple and the lesion centroid and the angular distance between the nipple-lesion centroid axis and the breast boundary on the current mammogram. In the present study, we compared the RRM to the use of warping techniques for the initial estimation of the lesion location. The current mammogram was warped by affine (AF) or thin plate splines (TPS) transformation in combination with simplex optimization in order to maximize a similarity measure between the breast areas on the current and prior mammograms. Correlation and mutual information (MI) similarity measures were evaluated. A set of 390 temporal pairs of mammograms containing biopsy-proven masses or microcalcification clusters was used. The true lesion locations were identified by an MQSA radiologist on all mammograms. 72 temporal pairs were used for training the parameters of the warping techniques. The remaining 318 pairs were used for testing the performance of the 5 methods. The registration accuracy was analyzed by evaluating the average distance between the centroids of the estimated and the true lesion locations on the prior mammogram.

RESULTS: The average distance between the estimated and the true lesion centroids on the previous mammogram after the initial stage was: RRM = 8.5 ± 6.2 mm, correlation-AF = 9.0 ± 6.7 mm, correlation-TPS = 10.3 ± 8.2 mm, MI-AF = 9.2 ± 7.5 mm, MI-TPS = 9.5 ± 8.6 mm. After the final

registration stage, the average distance between the estimated and the true centroids was: RRM = 6.4 ± 8.9 mm, correlation-AF = 7.0 ± 9.5 mm, correlation-TPS = 7.4 ± 10.2 mm, MI-AF = 6.9 ± 9.5 mm, MI-TPS = 7.2 ± 11.1 mm. **CONCLUSIONS:** The RRM method outperformed the warping techniques. It localized the corresponding lesions on temporal pairs of mammograms with the highest accuracy and the lowest standard deviation among the 5 methods.

379 • 11:30 AM

Observer Evaluation and CAD Performance of a Radial Gradient-based Segmentation Method for Mammographic Microcalcifications

S. Paquerault, PhD, Chicago, IL • L.M. Yarusso • R.M. Nishikawa, PhD • J. Papaioannou, MS • A.V. Edwards • Y. Jiang, PhD (paquerau@uchicago.edu)

PURPOSE: To perform an observer evaluation of the accuracy of a proposed segmentation method for microcalcifications in mammograms and to demonstrate the improvement in performance of our computerized classification scheme for malignant versus benign microcalcifications when using the proposed segmentation technique.

METHOD AND MATERIALS: We have implemented a radial gradient-based segmentation method for microcalcifications. It is difficult task for radiologists to manually outline the contours of each microcalcification. Therefore, we have conducted two observer studies to evaluate the proposed segmentation method. Two observers participated in each study, reviewing a database of 50 digitized mammograms with clustered microcalcifications. No observer participated in both studies. The first observer study (A) required each observer to rate the accuracies (0-100 scale) of both the proposed segmentation method and the one currently used in our computerized classification scheme. In the second observer study (B), each observer was asked to select their preferred method from three displayed segmentation methods: the proposed segmentation method, the watershed method and the current method. In these two studies, the original mammograms with no segmentation were also displayed. In addition, the 50 cases were randomly reviewed 2 to 3 times to analyze observers' consistencies. The effect of the proposed segmentation method on the performance of our computerized classification scheme was also investigated. ROC analysis was performed and the Az value was used as a performance index.

RESULTS: For study (A), the first observer gave accuracy ratings of 83 and 31 for the proposed and current segmentation methods respectively. The second observer also preferred the proposed method, with accuracy ratings of 92 versus 68 for the current method. For study (B), the observers selected the proposed method among the three displayed methods 56% and 62% of the time. Their other selections were equally distributed between the other two segmentation methods. The performance of the classification scheme improved when using the proposed segmentation method. The Az values for case-based performance were 0.84 with the proposed method versus 0.78 with the current method.

CONCLUSIONS: Two separate observer studies demonstrated that our proposed radial gradient-based segmentation technique for mammographic microcalcifications was preferred over other methods. The proposed method also improved the performance of our CAD classification scheme. (R.M.N., J.P. are shareholders in R2 Technology.)

380 • 11:40 AM

Computerized Mammographic Breast Density Estimation: Expectation-Maximization Estimation and Neural Network Classification of Breast Density

C. Zhou, PhD, Ann Arbor, MI • L.M. Hadjiiski, PhD • B. Sahiner, PhD • H. Chan, PhD • M.A. Helvie, MD • J. Wei, PhD (chuan@umich.edu)

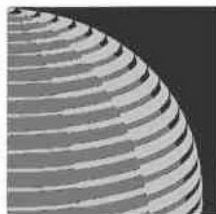
PURPOSE: Our previous study showed the feasibility of a rule-based automatic breast density estimation method. However, the rule-based technique could not classify the very fatty and very dense breasts consistently with high accuracy because some of these breasts have very similar gray level histograms. This study develops a new neural network (NN) classifier to improve the performance of rule-based breast density estimation.

METHOD AND MATERIALS: A mammogram is digitized and the pixel size is reduced to 0.8 mm. The breast region is first segmented by an automatic boundary tracking and a pectoral muscle trimming algorithm. An adaptive dynamic range reduction technique is used to reduce the range of the gray levels in the low frequency background and to enhance the separation of the gray levels of the dense and fatty regions. The breast images are first classified by a rule-based method into a class of median dense and a class of combined very dense/fatty breasts based on the characteristics of their gray level histograms. An Expectation-Maximization (EM) algorithm is then applied to the latter class to extract the gray level features. One morphological feature and 12 EM extracted gray level features are input to a feedforward neural network to further classify the mammograms in the combined class into a class of very dense breasts and a class of very fatty breasts. For each class, a gray level threshold is automatically estimated to segment the dense tissue. For comparison, an

Radiological Society of North America

RSNA'04

RADIOLOGY'S
GLOBAL
FORUM



Scientific Assembly and Annual Meeting Program

The Radiological Society of North America
90th Scientific Assembly and Annual Meeting
November 28 – December 3, 2004
McCormick Place, Chicago



RSNA

Radiological Society
of North America
Founded in 1915



American Association
of Physicists in Medicine

**Invited
Papers**

from ASNR, ASTRO, SIR
and SNM

Search

RSNA Meeting Program
rsna2004.rsna.org

dered an anatomic
p apnea (OSA) in
ion. Our purpose is
late in children with

es of the supraglot
OSA (20 with Down
The patients' soft
onically measured.
ade between three
own syndrome, and

a the soft palates of
OSA non-Down
(control 209.85, OSA
The differences in
OSA Down 318.33,
een the OSA groups

and increased signal
compared to normal
atomic cause of OSA

Pediatric Computed

ross@umc.edu)

ogy residents in the
in children, utilizing
resident interpreta-

children aged 1 day to
residents with 6-48
e in pediatric radiol-
recorded on an Agfa
pediatric radiologist,
l of severity; 4) false
reements were also
major (impacts clinical
omic regions.

ring of 2,484 thoracic,
musculoskeletal. Mean
pectively. Agreement
69 (17.3%), of which
1 level of agreement
then remained stable.
ncy (range = 9.7% to
t to 2nd year (7.8% to
region, agreement was
or disagreements were
atient age, agreement
ssive increase to 13%

dercall readings ex-
ately 2:1 ratio.
dercall the presence
interpretation rate of
Most improvement in
of residency.

esday Afternoon • Room S401AB

Physics (Mammography CAD)

ont sponsorship with the American Association of
icists in Medicine

BR MO HP PH

SPING: Nico Karssemeijer, PhD, Nijmegen, The Netherlands

Lubomir Hadjiyski, PhD*, Ann Arbor, MI

(N.K.: Research consultant and stockholder of R2
Technology, Inc.)

router Code: SSJ17 • 1 credit

one credit, relinquish attendance voucher at end of session.

17-01 • 3:00 PM

Computer-aided Detection (CAD) System for Improvement of Mass ection on Mammograms

PhD*, Ann Arbor, MI • B. Sahiner, PhD* • L.M. Hadjijski, PhD* • H.
PhD* • M.A. Helvie, MD* • M.A. Roubidoux, MD*

POSE: To develop a dual CAD system which combines a regular CAD
n with a new system trained with masses seen on retrospective
y of prior mammograms to improve its performance for detecting
masses.

METHOD AND MATERIALS: A data set of 109 patients containing 211
ent mammograms with biopsy-proven masses and 261 prior mammo-
ms was used. We randomly divided the data set into two independent
or both the current and prior mammograms: the training set
ained 54 cases and the test set contained 55 cases. Two single CAD
ms were trained, one with current mammograms and the other with
e mammograms. A two-stage gradient field analysis was used to
screen for mass candidates in both CAD systems. The suspicious
cture in each identified region was extracted by clustering-based
n growing. Morphological and spatial gray-level dependence texture
ures were extracted from the current mammograms. For detection of
subtle masses on the prior mammograms, histogram and run-length
sics features were extracted. Stepwise linear discriminant analysis
A) with simplex optimization was used to select the most useful
res. Finally, rule-based and LDA classifiers were used to differentiate
es from normal tissues. When the dual CAD system was applied to a
mammogram, the detection information by the two CAD systems on
ame mammogram were merged with a fusion scheme.

ULTS: When the single CAD system trained on current mammograms
plied to the test sets, the case-based sensitivities were 87% and 65%
current mammograms and 50% and 30% on prior mammograms at 2
FPs/image, respectively. When the single CAD system trained with
mammograms was used, the case-based sensitivities were 81% and
on current mammograms and 56% and 46% on prior mammograms at
1 FPs/image, respectively. With the dual CAD system, the case-
d sensitivities were improved to 89% and 75% on current mammo-
ms and 60% and 48% on prior mammograms at the same FP rates.

CONCLUSIONS: The dual CAD system improved the overall detection
ormance for all masses. Further work is underway to optimize the
n scheme in the dual CAD system.

17-02 • 3:10 PM

etermination of the Degree of Subjective Similarity for Pairs of Clustered ocalcifications on Mammograms: Preliminary Observer Study

uramatsu*, Chicago, IL • Q. Li, PhD* • R.A. Schmidt, MD • K. Suzuki,
* • G.M. Newstead, MD* • K. Doi, PhD (chisa@uchicago.edu)

POSE: Presentation of similar images should be useful for radiologists
e distinction between benign and malignant clustered microcalcifica-
s on mammograms. The purpose of this study was to determine
ologists' subjective similarity which could then be used as a gold
dard for evaluation of objective similarity measures for automated
e of similar images.

METHOD AND MATERIALS: A total of 884 (504 benign and 380 malig-
regions of interest (5 cm x 5 cm) for biopsy-proven clustered
ocalcifications was obtained from the Digital Database for Screening
mammography organized by the University of South Florida. An observer
y was conducted to obtain subjective similarity ratings for 114 pairs of
tered microcalcifications on mammograms. Six image pairs were
ed on a high resolution LCD monitor such that one image in the center
ompared to three images each on the right and left side. Pathologies
sions were not revealed to observers. Ratings were marked on a

continuous rating scale between 0 and 1, where 0 and 1 correspond to
images not similar at all and almost identical, respectively. Nine breast
radiologists, ten general radiologists, and nine non-radiologists partici-
pated in the study; some of them completed multiple times. Correlation
values between two observers, groups of observers, and individual
observers were determined.

RESULTS: Inter- and intra-observer correlation values varied from 0.021 to
0.602 and 0.408 to 0.721, respectively. Correlation values between two
breast radiologists were generally higher than those between two general
radiologists. When similarity ratings were averaged for breast radiologists
and general radiologists, the correlation value between the two groups
became 0.857, which is considered reasonably high.

CONCLUSIONS: The variation in similarity ratings between two individ-
als was not small. However, when a number of reliable observers provide
similarity ratings, average ratings may be used as a gold standard for
development of objective similarity measures to select similar images that
we expect will be useful for radiologists in the diagnosis of clustered
microcalcifications on mammograms, a task difficult for most radiologists.
(K.D.: Author is shareholder of Deus Technology Inc., Rockville, MD
K.D./R.A.S.: Authors are shareholders of R2 Technology Inc., Los Altos,
CA)

SSJ17-03 • 3:20 PM

Interval Change Analysis Based on Computerized Regional Registration of Corresponding Microcalcification Clusters on Temporal Pairs of Mammo- grams

L.M. Hadjijski, PhD*, Ann Arbor, MI • R. Chan, PhD* • B. Sahiner, PhD* • M.A.
Helvie, MD* • M.A. Roubidoux, MD* • C. Zhou, PhD* (lhadjisk@umich.edu)

PURPOSE: To develop an automated method for characterization of
microcalcification clusters using interval change information on serial
mammograms. This analysis will be useful for identification of new or
growing clusters in a detection system or for classification of malignant
and benign clusters in a diagnostic system.

METHOD AND MATERIALS: The automated interval change analysis
method consisted of two stages: (1) detection of corresponding cluster on
the prior, and (2) classification of cluster as new, growing, or stable. In the
first stage, based on the position of a detected cluster on the current
mammogram a regional registration procedure identified the local area
that might contain the corresponding cluster on the prior. A search
program was used to detect cluster candidates within the local area. The
cluster on the current mammogram was then paired with the detected
candidates to form (TP-TP) and (TP-FP) pairs. Features were automatically
extracted and a correspondence classifier was designed to reduce the false
pairs (TP-FP). In the second stage, the current cluster is classified as new if
no cluster is detected in prior, or the detected clusters will be classified as
growing or stable based on analysis of the current and prior pairs. In this
study, we focussed on the first stage. 175 serial mammogram pairs
containing biopsy-proven clusters on current mammograms were used.
An MQSA radiologist identified the corresponding clusters on the mammo-
grams. On priors, the radiologist rated 12 of the 175 clusters as not visible
and the subtlety of 18 clusters as 9 and 10 on a scale of 10. A leave-one-case-
out resampling scheme was used for feature selection and classification.

RESULTS: The search program detected 89% (156/175) of the clusters with
an average of 0.43 FP cluster on priors. The correspondence classifier
identified 81% (141/175) of the TP-TP pairs with 21 false matches within
the 162 image pairs that had detected clusters.

CONCLUSIONS: Our study demonstrated that our registration and match-
ing technique can find the corresponding cluster on the prior with high
sensitivity, considering many of the clusters were very subtle. This is a
promising step for automated analysis of clusters on serial mammograms.

SSJ17-04 • 3:30 PM

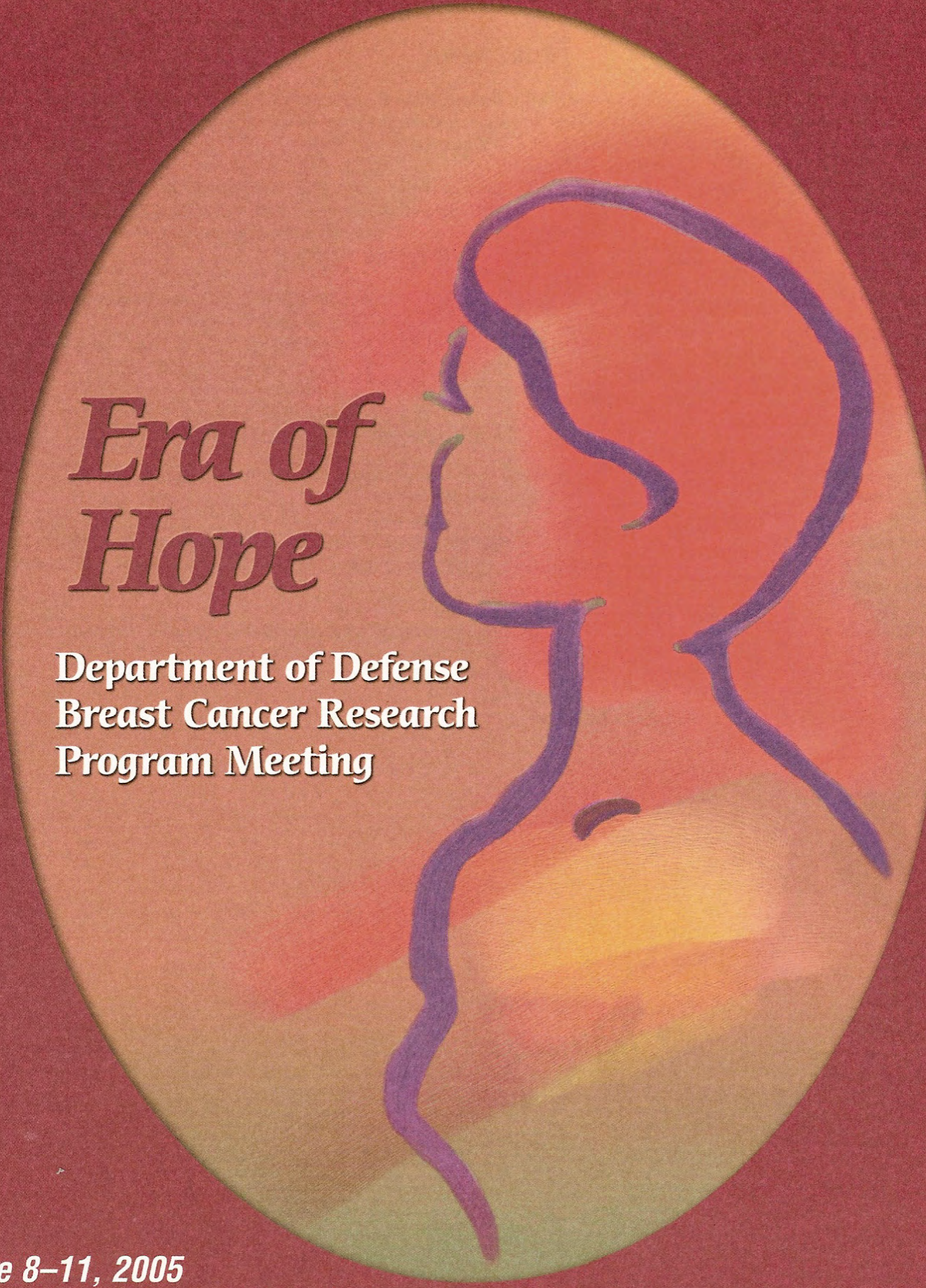
Computer-aided Diagnosis Scheme for Identifying Histological Classifica- tion of Clustered Microcalcifications Using MLO and CC Magnification Mammograms

(FDA)

R. Nakayama, MS*, Tsu-shi, Japan • Y. Uchiyama, PhD* • R. Watanabe, MD*
• S. Katsuragawa, PhD • K. Namba, MD* • K. Doi, PhD (nakayama@clin.medic
.mie-u.ac.jp)

PURPOSE: It is difficult to make correct clinical decisions for biopsy or
follow-up on clustered microcalcifications on mammograms. The purpose
of this study was to develop a computer-aided diagnosis scheme for
identifying histological classification of clustered microcalcifications on
magnification mammograms in order to assist radiologists' interpretation
as a "second opinion."

METHOD AND MATERIALS: Our database consisted of mediolateral
oblique (MLO) and craniocaudal (CC) magnification mammograms
(512x512 pixels, 12bit/pixels, 0.0275mm/pixel) obtained from 56 patients,
which included 38 malignant clustered microcalcifications (invasive carci-
noma, noninvasive carcinoma of comedo type, and noninvasive carcinoma



Era of Hope

Department of Defense
Breast Cancer Research
Program Meeting

*June 8–11, 2005
Pennsylvania Convention Center
Philadelphia, Pennsylvania*

PROCEEDINGS

nostic process, we have developed a display system for efficiently presenting information about changing tissue patterns, derived from longer mammographic histories.

The system provides for: (1) Deforming mammograms so that all images geometrically match the form of the corresponding view in the most recent exam; (2) Correcting for differences in exposure between exams; (3) Measuring local trends in various parameters over time and representing these trends in summary images; and, (4) Displaying the normalized mammographic images in a cine mode, along with summary images. The parameters that have been implemented to date are local breast density and local variance of pixel values, which provide a general prototype mechanism for other parameters to be added in the future.

The fully automatic geometric transform can map any mammographic image onto a reference image while guaranteeing registration of specific features and maintaining grayscale equivalence. A polar coordinate system is established with its origin at the intersection of the nipple axis with the pectoral muscle. A tissue pixel is identified by coordinates consisting of: (1) a relative distance between the origin and skin line; and (2) its angle relative to the nipple axis. Pixels are mapped onto a position in a reference image determined by these relative coordinates. This transformation guarantees that pectoral lines, nipples and skin lines are all placed in complete registration. Images are then adjusted by converting film density to log-exposure and dividing by the Jacobian of the geometric transformation to correct for local expansion factors. Relative exposures are equalized with respect to the reference image by applying linear regression to adjust corresponding pixel value pairs.

After this normalization process, each image in a sequence is processed by two feature-detection filters that measure local tissue density and local variance at each point. To measure local density, the fraction of fibroglandular tissue projected onto each pixel is determined and represented in an image, which is then convolved with a Gaussian kernel. At each location, trends over time in parameters are calculated and represented in summary images. For each parameter, the slope of its regression line, and its variance with respect to its regression line, are mapped onto a 2D color scale.

For subjective evaluation by radiologists, the system has been loaded with 240 verified cases for which we have at least three screening exams; however, an overall objective evaluation of the system is not within the scope of the current project.

The U.S. Army Medical Research and Materiel Command under DAMD17-02-1-0549 supported this work.

P14-5: INTERVAL CHANGE ANALYSIS OF CORRESPONDING CLUSTERED MICROCALCIFICATIONS ON SERIAL MAMMOGRAMS BASED ON AUTOMATED REGIONAL REGISTRATION

Lubomir M. Hadjiiski, Ph.D., Heang-Ping Chan, Ph.D., Berkman Sahiner, Ph.D., Mark A. Helvie, Marilyn A. Roubidoux, and Chuan Zhou, Ph.D.
Department of Radiology, University of Michigan, Ann Arbor, MI
E-mail: lhadjisk@umich.edu

Our goal is to develop an automated method for characterization of microcalcification clusters using interval change information on serial mammograms. This analysis will be useful for identification of new or growing clusters in a computer-aided detection system or for classification of malignant and benign clusters in a computer-aided diagnosis system.

The automated interval change analysis method consisted of two stages: (1) detection of corresponding cluster on the prior, and (2) classification of cluster as new, growing, or stable. In the first stage, based on the position of a detected cluster on the current mammogram, a regional registration procedure identified the local area that might contain the corresponding cluster on the prior. A search program was used to detect cluster candidates within the local area. The cluster on the current mammogram was then paired with the detected candidates to form (TP-TP) and (TP-FP) pairs. Features were automatically extracted and a correspondence classifier was designed to reduce the false pairs (TP-FP). In the second stage, the current cluster was classified as new if no cluster was detected on the prior, or the detected clusters would be classified as growing or stable based on analysis of the current and prior pairs. A linear discriminant classifier with stepwise feature selection was used to merge and select the optimal feature subset. 175 serial mammogram pairs containing biopsy-proven clusters on current mammograms were used in this study. An MQSA radiologist identified the corresponding clusters on the mammograms as gold standard. On priors, the radiologist rated 12 of the 175 clusters as not visible and the subtlety of 18 clusters as 9 and 10 on a scale of 10 (10=subtlety). A leave-one-case-out resampling scheme was used for feature selection and classification.

Using a search region with an average area of 1401 mm² allowed all clusters of interest to be localized in the search region. The average distance between the estimated and the true centroid of the clusters on the prior mammogram was 7.95±4.73 mm. The search program detected clusters on 164 of the priors, including 90.3% (158/175) of the true clusters with an average of 0.43 FP clusters/image. The correspondence classifier identified 84% (147/175) of the TP-TP pairs with 17 false matches. The temporal

malignant-benign classifier achieved an Az of 0.83±0.03. For comparison, the classifier based on the current mammograms alone achieved an Az of 0.79±0.04.

The study demonstrates that our registration and matching techniques can identify the corresponding cluster on the prior with high sensitivity, considering many of the clusters were very subtle. The malignant-benign classifier successfully merged the current and prior information extracted from the automatically detected clusters. It also achieved higher accuracy than the classifier based on current information alone. This is a promising step towards automated analysis of clusters on serial mammograms.

The U.S. Army Medical Research and Materiel Command under DAMD17-02-1-0489 supported this work.

P14-6: MASS SEGMENTATION OF DENSE BREASTS ON DIGITIZED MAMMOGRAMS

L. Kinnard,^{1,2} S.-C. B. Lo,² E. Duckett,³ E. Makariou,² M. T. Freedman,² and M. Choukha¹

¹Department of Electrical and Computer Engineering, Howard University, Washington, DC; ²Imaging Science and Information Systems Center, Georgetown University Medical Center, Washington, DC; ³Advanced Radiology, Glen Burnie, MD
E-mail: kinnard@isis.imac.georgetown.edu

In this study a segmentation algorithm based on steepest changes of a probabilistic cost function is tested on non-processed and pre-processed dense breast images in an attempt to determine the efficacy of pre-processing for dense breast masses. The pre-processing method is a background trend correction (BTC) technique.

The segmentation method used in this study evaluates the steepest changes within a probabilistic cost function in an effort to determine the computer segmented contour which is most closely correlated with expert radiologist manual traces. This method segments breast masses by combining region growing with probability-based function analysis. Based on this analysis the three best contours are chosen and a final selection is made from these three choices. Typically, the Group 1 trace encapsulates the central portion of the mass, the Group 2 trace encapsulates the central mass and borders extending into surrounding tissue (e.g., spiculations), and the Group 3 trace encapsulates the area covered by the Group 2 trace and surrounding fibroglandular tissue. The BTC method alters intensity values of the Region of Interest (ROI) using a polynomial fitting function. This method was tested on 71 dense cancerous masses. The computer-segmented results were manually traced by two expert radiologists for validation purposes. The overlap (O), accuracy (A), sensitivity (SE), specificity (SP), and Dice Similarity Coefficient (DSC) statistics were calculated, where a DSC value greater than 0.7 implies strong agreement between the computer segmented result and the expert radiologist trace. Tables 1-2 contain mean values for all statistics, and Figures 1-2 show computer segmented results.

Generally, the BTC method worsened the computer segmented results for Experts A and B regarding overlap, DSC, and sensitivity statistics. These results conflict with visual inspection of the BTC processed ROI's because this method sometimes creates a crater-like effect around the mass borders in areas where it was formerly difficult to separate mass borders from surrounding tissue. Further, some light areas are lightened by background trend correction which causes areas outside the mass to be joined with areas inside the mass. This phenomenon subsequently causes the region to grow too much. We feel that the computer-segmentation results can be improved by changing the parameters used to determine the intensities that will produce the contours that best match expert radiologist traces. The purpose of this work is to facilitate breast cancer screening using digitally automated segmentation method capable of locating mass borders embedded in dense breasts.

Table 1 – Statistical Results for Non-Processed and Processed ROI's (Expert A)

	EXPERT A (NON-PROCESSED ROI)					EXPERT A (BTC PROCESSED ROI)				
	O	A	SE	SP	DSC	O	A	SE	SP	DSC
Group 1	0.3	0.73	0.32	0.98	0.44	0.18	0.71	0.19	1	0.28
Group 2	0.46	0.78	0.56	0.93	0.6	0.34	0.76	0.36	0.99	0.46
Group 3	0.47	0.77	0.63	0.88	0.64	0.34	0.75	0.44	0.95	0.49

Table 2 – Statistical Results for Non-Processed and Processed ROI's (Expert B)

	EXPERT A (NON-PROCESSED ROI)					EXPERT A (BTC PROCESSED ROI)				
	O	A	SE	SP	DSC	O	A	SE	SP	DSC
Group 1	0.38	0.82	0.4	0.97	0.52	0.26	0.83	0.27	1	0.38
Group 2	0.52	0.84	0.65	0.91	0.66	0.44	0.86	0.49	0.99	0.57
Group 3	0.48	0.81	0.72	0.86	0.63	0.41	0.84	0.57	0.94	0.57



RSNA2005

Connecting for Lifelong Learning

Radiological Society of North America

Scientific Assembly and Annual Meeting Program

Radiological Society of North America

91st Scientific Assembly and Annual Meeting

November 27 – December 2, 2005

McCormick Place, Chicago



RSNA

Radiological Society
of North America
Founded in 1915



American Association
of Physicists in Medicine

Invited Papers from ASNR, ASTRO, SIR and SNM
Search the RSNA Meeting Program
at rsna2005.rsna.org

tion. Also, for each observer, sensitivity and specificity were determined from all 3 types of interpretations. Paired t-tests were performed to determine the significance of differences in the average sensitivities and specificities without and with CAD.

RESULTS: For both BIRADS and CR, it was not possible for every observer to choose a cutoff that resulted in a PMD that was in agreement with the actual PMD. However, use of user-dependent cutoffs resulted in better agreement than use of constant cutoff. Without the use of CAD, the averages over all observers of the sensitivity/specificity pair as determined from PMD, BIRADS, CR (2% cutoff), CR (a user dependent cutoff) were 0.88/0.66, 0.86/0.70, 1.00/0.03, and 0.93/0.46, respectively. With the use of CAD, the average sensitivity/specificity pairs were 0.93/0.67, 0.92/0.77, 1.00/0.04 and 0.95/0.56, respectively.

CONCLUSIONS: For many users, different forms of radiologists' interpretations result in different patient management decisions. Different forms of radiologists' interpretations may also result in different conclusions about the ability of CAD to improve the radiologist performance. Finally, when determining patient management from confidence ratings, user-dependent cutoffs are needed. (K.J.H., M.L.G., C.E.M.: Shareholders in R2 Technology, Inc. (Los Altos, CA).)

SSC17-05 • 11:10 AM

Computer-aided Diagnosis Scheme for Identifying Histological Classification of Clustered Microcalcifications Using Follow-up Magnification Mammograms

R. Nakayama, PhD*, Tsu, Japan • R. Watanabe, MD* • K. Namba, MD* • K. Takeda, MD* • S. Katsuragawa, PhD • K. Doi, PhD • et al (nakayama@clin.med.mie-u.ac.jp)

PURPOSE: The histological classification of clustered microcalcification on mammograms can be difficult, and thus often requires follow-up. The purpose of this study was to develop a computer-aided diagnosis scheme for identifying histological classification of clustered microcalcifications on follow-up magnification mammograms in order to assist radiologists' interpretation as a "second opinion."

METHOD AND MATERIALS: Our database consisted of 186 magnification mammograms which included current and previous images obtained from 93 patients after three months follow-up. It included 11 invasive carcinomas, 19 noninvasive carcinomas of comedo type, 25 noninvasive carcinomas of noncomedo type, 23 mastopathies and 15 fibroadenomas. The histological classifications of all clustered microcalcifications were proved by pathologic diagnosis after three months follow-up. The clustered microcalcifications were first segmented by use of a filter bank and a thresholding technique. Five objective features on clustered microcalcifications were determined from each of current and previous images by taking into account subjective features that experienced radiologists commonly use to identify possible histological classifications. Bayes discriminant function was employed for distinction between five histological classifications. For the input of Bayes discriminant function, we used five objective features obtained from current images, and also ten objective features obtained from both current and previous images.

RESULTS: With current images, the classification accuracy ranged from 76.0% to 90.9%, but was improved substantially by use of previous images. With ten objective features, the classification accuracies of our computerized scheme were 100% (11/11) for invasive carcinoma, 100% (19/19) for noninvasive carcinoma of comedo type, 96.0% (24/25) for noninvasive carcinoma of noncomedo type, 95.7% (22/23) for mastopathy, and 100% (15/15) for fibroadenoma.

CONCLUSIONS: By use of both current and previous images, this computerized scheme achieved high classification accuracies, and would be useful to assist radiologists in their assessment of clustered microcalcifications. (S.K., K.D. are shareholders in R2 Technology.)

SSC17-06 • 11:20 AM

Automated Regional Registration and Classification of Corresponding Microcalcification Clusters on Serial Mammograms

L.M. Hadjiliski, PhD*, Ann Arbor, MI • H. Chan, PhD* • B. Sahiner, PhD* • M.A. Helvie, MD* • M.A. Roubidoux, MD* • C. Zhou, PhD* (lhadjiliski@umich.edu)

PURPOSE: To develop an automated system for detecting corresponding microcalcification clusters on serial mammograms, and classifying the cluster as malignant and benign using interval change information.

METHOD AND MATERIALS: Our system consists of two stages. In the first stage, based on the location of a detected cluster on the current mammogram, a regional registration procedure identifies the local area on the prior that may contain the corresponding cluster. A search program is used to detect cluster candidates within the local area. The cluster on the current image is then paired with the candidates to form true (TP-TP) or false (TP-FP) pairs. A correspondence classifier using automatically extracted features is designed to reduce the false pairs. In the second stage, a temporal classifier based on current and prior information is used if a cluster is detected in the prior, and a current classifier based on current

information alone is used if no prior cluster is detected. In this study, 175 serial pairs containing biopsy-proven calcification clusters were used. An MQSA radiologist identified the corresponding clusters on the mammograms. On the priors, the radiologist rated 12 of the 175 clusters as not visible and the subtlety of 18 clusters as 9 or 10 on a scale of 10. Leave-one-case-out resampling was used for feature selection and classification.

RESULTS: The search program detected 90.2% (158/175) of the clusters on the priors with an average of 0.43 FPs/image. The correspondence classifier identified 85% (149/175) of the TP-TP pairs with 15 false matches within the 164 image pairs that had detected clusters. In the classification stage the temporal classifier achieved a test Az of 0.83 for the 164 pairs for classifying the clusters as malignant or benign. For the 11 clusters without detection on the prior, the test Az by the current classifier was 0.72. In comparison, the MQSA radiologist achieved an Az of 0.72 for both the 175 and the 164 temporal pairs.

CONCLUSIONS: Our interval change analysis system can detect the corresponding cluster on the prior mammogram with high sensitivity, and classify them with an accuracy comparable to that an experienced radiologist.

SSC17-07 • 11:30 AM

Workflow Analysis for a Clinical Breast Ultrasound CAD Workstation Prototype

N. Gruszkas*, Chicago, IL • K. Drukker, PhD* • C.A. Serinett, MD* • L. Lan, MS* • M.L. Giger, PhD • I. Bonta, MD* (ngrusz1@uic.edu)

PURPOSE: To evaluate the impact of a prototype breast ultrasound CAD workstation on the workflow in a clinical environment, including its integration with standard RIS equipment and its use by radiologists.

METHOD AND MATERIALS: We designed a breast ultrasound CAD prototype workstation to be utilized in a clinical setting based on previous experience with retrospective image analysis using CAD methodology. In its current implementation, the workstation is configured as an archive destination on our clinical ultrasound scanner, an HDI 5000 by Philips Medical Systems. We designed an automatic image transfer method using DICOM protocols to transfer images directly from the scanner to the workstation. There, the images are automatically preprocessed and all patient-identifiable information is removed using in-house developed software. The radiologist then performs lesion identification on each image using our customized graphical user interface. For the purposes of this workflow study, CAD analysis results were not displayed in order to prevent influence of patient care. Using our prototype workstation, images from 40 patients - who consented to participate in this study - were obtained from exams performed by a single radiologist. The radiologist was surveyed to determine the workstation's overall impact on clinical workflow.

RESULTS: Our workstation design was able to completely interoperate with the clinical DICOM-compliant equipment. The amount of time necessary to transfer an entire exam to the workstation varied substantially. However, the radiologist reported that the workstation added only one to two minutes to the amount of time necessary to perform a standard ultrasound workup.

CONCLUSIONS: The use of our prototype workstation has no significant impact on the time required to perform a standard diagnostic breast ultrasound exam and on the clinical workflow in general. Our design allows for easy integration into a standard clinical environment due to its utilization of industry standard DICOM protocols. (M.L.G.: M. L. Giger is a shareholder in R2 Technology, Inc (Sunnyvale, CA). It is the policy of the University of Chicago that investigators disclose publicly actual or potential significant financial interests that may appear to be affected by the research activities.)

SSC17-08 • 11:40 AM

Volumetric Breast Density Estimation from Full Field Digital Mammograms

N. Karssemeijer, PhD*, Nijmegen, Netherlands • S. van Engeland* • C. Boetes, MD* • H. Huisman, PhD* • P. Snoeren, PhD*

PURPOSE: Breast density is an important risk factor for breast cancer. The purpose of this paper is to present a method for accurate estimation of volume of dense breast tissue from full field digital mammograms (FFDM) and to validate results by correlation with volumes of dense breast tissue determined from breast MRI.

METHOD AND MATERIALS: Unprocessed FFDM images allow conversion of pixel values to the log exposure domain. By using a physical model of image acquisition this allows estimation of the proportion of dense breast tissue contributing to each pixel. By integration, the volume of dense tissue can be obtained. The physical model we use is based on the assumption that the breast is composed of two types of tissue, fatty and dense. Effective linear attenuation coefficients of these tissues were derived from empirical data as a function of three parameters: Tube voltage (kVp), anode material, and filtration. These parameters are available from the DICOM image headers. A simple relation is derived that allows computa-

RSNA

2006

Strengthening
Professionalism



Radiological Society of North America

Scientific Assembly and Annual Meeting Program 2006



Radiological Society of
North America

92nd Scientific Assembly and Annual Meeting
November 26 – December 1, 2006
McCormick Place, Chicago

- **New** Multisession Course section, pp 79–126
- **Search** the RSNA Meeting Program at rsna2006.rsna.org

RSNA

Radiological Society
of North America
Founded in 1915



American Association
of Physicists in Medicine

with the lesion outline - as indicated by a radiologist - was larger than 0.4, or the center of the region was located within the lesion outline. A combination of a rule-based approach and a neural network was used to classify regions as true or false positive. The evaluation was performed using a Round-Robin (leave-one-out-by-case) approach. It is important to note that this computerized method requires no human input.

RESULTS: For 90% of the actual lesions a true positive region was identified. In the task of distinguishing regions corresponding to actual lesions from those corresponding to normal breast tissue, an area under the ROC curve of 0.94 was obtained. In FROC analysis, an overall lesion detection sensitivity of 80% (on a per image basis) was obtained at the rate of 1 false-positive region per image. Moreover, at this operating point, 42% of the images had no false-positives.

CONCLUSION: The promising performance in this preliminary study of our new computerized method for lesion detection on breast ultrasound warrants further exploration and clinical translation of this method.

SSC17-03 • 10:50 AM

Multi-category Feature Extraction in Computer-aided Diagnosis of Breast MRI

W. Chen, MS*, Chicago, IL • M.L. Giger, PhD* • G.M. Newstead, MD* • U. Bick, MD • L. Lan • S. Arkani-Hamed • et al (weijie@uchicago.edu)

CLINICAL RELEVANCE/APPLICATION: Our image processing techniques has potential to improve the efficiency and effectiveness of breast MRI interpretation.

PURPOSE: Clinical consensus shows that both kinetic and morphological features on breast MRI are useful and should be combined in interpretation of breast MRI. We are developing computerized methods for automatic extraction of multi-category lesion features from 4D MRI datasets.

METHOD AND MATERIALS: Breast MR images were obtained with a T1-weighted SPGR sequence using Gd-DTPA. Each case has one precontrast and 5 postcontrast series and each series contains 60 coronal slices. The first database (77 malignant and 44 benign) was from a 1.5T Siemens scanner with a temporal resolution of 69s. The second database (109 malignant and 51 benign) was from a 1.5T GE scanner with a temporal resolution of 72s. In our automatic method, the breast lesions initially undergo 3D segmentation by the computer. Then, a fuzzy c-means clustering based method is employed to identify the most-enhancing kinetic curve from the lesion and kinetic features (time to peak, uptake rate, and washout rate) are extracted. To quantify the spatial properties of contrast uptake heterogeneity, texture features are extracted using a 3D gray-level co-occurrence matrix (GLCM) method. Finally, shape descriptors (circularity and irregularity) are calculated to quantify the tumor shape. The performance of these features in the task of distinguishing between malignant and benign lesions was assessed using ROC analysis.

RESULTS: All the three categories of features are found to be useful in differential diagnosis, with Az values of individual features ranging from 0.6 to 0.8. The performance of kinetic features from the most-enhancing curve was found to be significantly better than that from averaging over the entire lesion ($p=0.02$). The performances of texture features from 3D analyses were found to be significantly better than those from 2D analyses ($p<0.001$).

CONCLUSION: In designing a CAD system for breast MRI, both kinetic and morphological features should be considered. Kinetic features should be extracted from the most-enhancing regions and it is advantageous to extract morphological features in 3D lesion instead of from one 2D slices.

SSC17-04 • 11:00 AM

ROC Study: Effects of Computer-aided Diagnosis on Radiologists' Characterization of Malignant and Benign Breast Clustered Microcalcifications in Temporal Pairs of Mammograms

L.M. Hadjiiski, PhD, Ann Arbor, MI • H. Chan, PhD • B. Sahiner, PhD • M.A. Roubidoux, MD • M.A. Helvie, MD • C.P. Paramagul, MD • et al (lhadjisk@umich.edu)

CLINICAL RELEVANCE/APPLICATION: CAD using interval change analysis may increase the positive predictive value of mammography.

PURPOSE: To evaluate the effects of computer-aided diagnosis (CAD) on radiologists' characterization of clustered microcalcifications on serial mammograms.

METHOD AND MATERIALS: We developed an automated CAD system to register and classify microcalcification clusters as malignant or benign based on interval change information on serial mammograms. In this study, we conducted observer performance experiments with receiver operating characteristic (ROC) methodology to evaluate the effects of CAD on radiologists' estimates of the likelihood of malignancy (LM) of the clusters. 175 pairs of serial mammograms from 65 patients containing clustered microcalcifications (51 malignant and 124 benign) were chosen from patient files with IRB approval. The true cluster locations were identified by an MQSA radiologist on all current mammograms and 164 of the priors. Regions of interest containing the corresponding clusters were

extracted from the current and prior mammograms of each pair and analyzed by the CAD system. All cases eventually underwent biopsy so that interval change was observed for most of the clusters even if they were found to be benign after biopsy. This was therefore a difficult data set for interval change analysis. Four MQSA radiologists, different from the one who identified the clusters, assessed the temporal pairs that were displayed side-by-side on a workstation. The cases were read in a counter-balanced design. The readers provided estimates of the LM and BI-RADS assessment without and then with CAD. The classification accuracy was quantified by the area under ROC curve, Az.

RESULTS: The CAD system alone achieved a test Az value of 0.83 for this data set. For the four radiologists, the average Az in estimating the LM was 0.70 (range: 0.64-0.75) without CAD and improved to 0.77 (range: 0.68-0.83) with CAD. The improvement was statistically significant ($p=0.04$).

The ROC study is ongoing to include additional radiologists as observers. **CONCLUSION:** CAD using interval change analysis can significantly improve radiologists' accuracy in classification of clustered microcalcifications on serial mammograms.

SSC17-05 • 11:10 AM

Conversion of Screen Film Mammographic CADx for FFDM

H. Li, PhD, Chicago, IL • M.L. Giger, PhD* • Y. Yuan, BS • C.A. Sennett, MD • L. Lan • A.R. Jamieson, BA • et al (huili@uchicago.edu)

CLINICAL RELEVANCE/APPLICATION: Our analysis was performed on clinical FFDM cases, thus we expect that our CADx methods will be translated to the clinical arena to aid clinicians on diagnostic decisions and integration with PACS.

PURPOSE: We have developed computerized methods for the analysis of mammographic lesions to aid in the diagnosis of breast cancer. Our earlier development was performed on digitized screen-film mammograms. The purpose of this research is to convert and optimize our existing computerized methods and evaluate these methods on full-field digital mammography (FFDM) image for the classification of breast lesions.

METHOD AND MATERIALS: Our computerized method involves three major automatic steps: 1) segmentation of the lesion from parenchymal background using region growing, radial gradient index (RGI), and active contour snake techniques; 2) calculation of mathematical descriptors to describe lesion characteristics; and 3) merging of lesion features into an estimate of the probability of malignancy using linear discriminant analysis. The performance of individual features and the probability of malignancy (merged feature) were evaluated using ROC analyses. The FFDM images used in this study were collected with a GE Senographe 2000D system. The dataset contained 148 malignant lesions (412 images) and 139 benign lesions (327 images).

RESULTS: From round-robin analysis, by using radiologist-delineated lesion margins as "truth" at overlap threshold cutoff of 0.6, Az values of 0.83, 0.79, and 0.78 (and partial Az values of 0.43, 0.38, and 0.33) were obtained for the merged features, for the region growing, RGI and active contour snake segmentation techniques, respectively. We failed to show a statistical difference in these performance values, indicating that the computer analysis was not sensitive to our three segmentation methods. In particular, we found that contrast features were less sensitive to the accuracy of lesion segmentation than our spiculation features.

CONCLUSION: Using our developed computerized methods, our preliminary study shows promising results for breast lesion classification on FFDM images.

SSC17-06 • 11:20 AM

Model-free Analysis of MR Image Time-Series: How Many Clusters Should be Used?

A. Wismueller, MD, PhD, Munich, Germany • A. Meyer-Baese, PhD • O. Lange, PhD • G. Leinsinger • M.K. Hurdal, PhD • M.F. Reiser, MD • et al (awismueller.de)

CLINICAL RELEVANCE/APPLICATION: To determine the optimal number of clusters is a frequently neglected, yet important step to appropriate model-free MR image time-series analysis.

PURPOSE: Model-free clustering methods for MR image time-series analysis are increasingly used as an alternative to classical model-based methods, such as cross-correlation or statistical regression. But how many clusters should be used? The aim was to analyze this so-called Cluster Validity (CV) problem for MRI time-series analysis.

METHOD AND MATERIALS: Image time-series were acquired from a functional MR experiment performed in 6 healthy volunteers on a 1.5 T system (GE-EPI, TR/TE=4000/66 ms) in a 64 scan visual stimulation setting. The time-series vectors were clustered by minimal free energy vector quantization (MFE-VQ) (Wismueller et al, Int J Comp Vision 46(2)). Three CV indices known from the pattern recognition literature were computed on the results obtained by 20 runs of MFE-VQ on each data set, namely Kim's index (KI), Calinski & Harabsz index (CHI), and the intraclass index (ICI). For quantitative evaluation, the maximal correlation c of the consistently task-related component with the reference function

LL-PH5154

Multimodality Image Registration Based on Normalized Mutual Information Incorporated with Spatial Information

X. Yang, Suita, Japan • T. Soma • K. Murase, PhD

PURPOSE/AIM OF THE EXHIBIT: (1) To review multimodality image registration based on normalized mutual information (NMI) (2) To implement image registration based on NMI combined with spatial information (3) To investigate the effect of standard deviation σ of a gaussian filter on the accuracy of NMI-based registration in various noisy cases using simulated MRI and PET.

CONCLUSION/SUMMARY: The major teaching points of this exhibit are: (1) NMI combined with spatial information is a robust method for registration. (2) Removing noise in preprocessing step is also necessary to improve the accuracy of the above registration although with better robustness. (3) Reasonable selection of σ of the gaussian filter can improve the accuracy of registration in various noisy cases.

LL-PH5155

Computer-aided Characterization of Malignant and Benign Breast Clustered Microcalcifications on Serial Mammograms: Early Experience of Its Effects on Radiologists' Performance from an ROC Study

L.M. Hadjiiski, PhD, Ann Arbor, MI • H. Chan, PhD • B. Sahiner, PhD • A.V. Nees, MD • J.E. Bailey, MD • S.K. Patterson, MD • et al (lhadjiski@umich.edu)

PURPOSE/AIM OF THE EXHIBIT: (1) To understand the design of an observer performance study for characterization of microcalcification clusters on serial mammograms without and with CAD. (2) To understand the effects of CAD on radiologists' assessment of the likelihood of malignancy (LM) of clustered microcalcifications.

CONCLUSION/SUMMARY: CAD using interval change analysis may be useful for assisting radiologists in classification of microcalcification clusters and thereby reducing benign biopsies. This exhibit will lead to understanding of (1) Design of a CAD system using interval change analysis. (2) Design of an observer performance study for evaluation of CAD using receiver operating characteristic (ROC) methodology. (3) Interaction of observer with a CAD system (4) Effects of CAD on radiologists' decision.

LL-PH5156-D (Monday • 12:15 PM)

CT Dosimetry: A Comparison of Measurement Techniques and Devices

T.J. Vrieze, RT(R), Rochester, MN • M.R. Bruesewitz, RT(R) • A. Primak, PhD • J. Zhang, PhD • C.H. McCollough, PhD (mccollough.cynthia@mayo.edu)

PURPOSE/AIM OF THE EXHIBIT: 1) To review the differences between the measurement of dose to a point and the CT Dose Index (CTDI). 2) To describe current techniques and devices for measuring both absolute point dose and CTDI. 3) To summarize surface dose measurements for interventional and perfusion CT, where the CTDI construct is not directly applicable.

CONCLUSION/SUMMARY: The teaching points of this exhibit are: 1) The use of "small" dosimeters (e.g. RTI CT Slice Profile probe, Farmer chambers, MOS-FET devices, TLD or OSL chips) enables accurate point dose measurements in CT, which are necessary to determine surface or organ doses from interventional and perfusion exams. For these exams, CTDI100 can overestimate surface dose by a factor of 2 or more. 2) Surface CTDI100 values are reasonable estimates of surface dose for sequential and spiral exams

LL-PH5157

Pediatric CT: Set-up of a Dose Optimization Process

F.R. Verdun, PhD, Lausanne, Switzerland • D. Gutierrez, MS • C. Schlapoutaki, MD • P. Schnyder, MD • F. Gudinchet, MD (Francis.Verdun@chuv.ch)

PURPOSE/AIM OF THE EXHIBIT: To present a methodology to set-up diagnostic reference levels (DRL) in pediatric CT on the basis of our own experience. It is intended to explicit the CT dose indicators (CTDI, DLP, dose efficiency parameters) and the concept of DRL. The exhibit will also discuss the over-ranging problematics and the potential of automatic exposure devices.

CONCLUSION/SUMMARY: The main difficulty to set-up DRL is the understanding of the CT dose indicator. Our experience have shown that a simple presentation allows to organise a dosimetric survey by means of questionnaires in a reliable way. Our DRL will be compared with published data and will provide radiologists with values that might help them to reconsider their acquisition protocols. Finally, these results will help radiologists to set the automatic exposure parameters in order to spare as much as possible dose

LL-PH5158

New Concept for Dose Modulation at Multidetector-Row CT: Optimization of Radiation Dose Based on Contrast-to-Noise Ratio

T. Goto, Kashiwa, Japan • K. Hirokawa • Y. Sugaya, MA • O. Miyazaki • Y. Funama, PhD • Y. Yamashita, MD • et al

PURPOSE/AIM OF THE EXHIBIT: The purpose of this exhibit is to propose a new dose modulation technique based on Contrast-to-Noise Ratio (CNR), which can reduce the radiation dose by optimizing both the tube current (mA) and voltage (kV).

CONCLUSION/SUMMARY: By using the CNR-based dose modulation, further dose reduction can be achieved as compared with the SD-based dose modulation. The major teaching points of this exhibit are: A. The optimal setting of x-ray B. Principle and characteristic of CNR-based dose modulation.

LL-PH5159

Automated Segmentation and Volumetry of the Whole and Each Region of the Liver on CT Images

N. Hayashi, Kanazawa, Japan • T. Takata, RT • S. Sanada, PhD • M. Suzuki, MD • H. Tsujii • O. Matsui, MD • et al (hayashi@sanadalab.com)

PURPOSE/AIM OF THE EXHIBIT: For living donor liver transplantation, it is important to measure the volume of the whole liver and the segment liver which is excised on CT images. The purpose of this exhibit is to describe how to segment and measure the whole and segment liver volume automatically.

CONCLUSION/SUMMARY: It is difficult to analysis enormous MDCT data without computer assist. This technique is easy-to-use and can analyze correctly in clinical use. This exhibit reviews A) the methods of automated segmentation of the liver and hepatic veins on CT images B) the method of automated segmentation of each region of the liver using information of the hepatic veins C) the comparison of the volume between automated segmentation and manual segmentation

LL-PH5160

Dual-Source Computed Tomography: How Does It Work and What Can It Do?

M.R. Bruesewitz, RT(R), Rochester, MN • C.H. McCollough, PhD • H. Bruder, PhD • B. Schmidt, PhD • R. Raupach, PhD • T.G. Flohr, PhD (mccollough.cynthia@mayo.edu)

PURPOSE/AIM OF THE EXHIBIT: 1) To describe the design of the 64-Slice Dual-Source CT scanner. 2) To explain the value of Dual-Source CT for cardiac imaging. 3) To identify potential applications of Dual-Source CT including dual energy and bariatric imaging.

CONCLUSION/SUMMARY: The major teaching points of this exhibit are: 1) The use of two x-ray tubes and two detection systems, mounted orthogonally on a single gantry, allows for a factor of 2 improvement in temporal resolution, while maintaining or lowering dose for cardiac CT 2) Dual-Source CT enables the simultaneous acquisition of dual-energy CT data for material-selective imaging (each tube at a different kV), or can operate two tubes at the same kV to improve the imaging of morbidly-obese patients

LL-PH5161

Can CT Go with the Flow? Measuring Blood Velocity with Volume and Rotational CT

J.A. Anderson, PhD, Dallas, TX • G.M. Arbique, PhD • L.M. Alhilali, MD • D.P. Chason, MD • D.H. Uhrbrock, MD • T.J. Lane, PhD (jon.anderson@outsouthwestern.edu)

PURPOSE/AIM OF THE EXHIBIT: 1) Review x-ray angiographic methods for measuring blood flow velocities. 2) Discuss the potential of current volume CT and rotational (C-arm) CT for blood flow velocity measurements at different anatomical sites. 3) Illustrate velocity measurement approaches with phantom studies.

CONCLUSION/SUMMARY: 1) Blood velocity measurements can complement CT or angiographic studies, but determining these values with x-ray modalities is not yet available in clinical practice. 2) Current capabilities of volume CT scanners and of rotational angiographic equipment may allow flow velocities to be obtained in clinical settings. 3) The use of these techniques may provide velocity data with high quality anatomical images for improved diagnosis of vascular disease.

Abstract ID: 5016138**Submission Type: Scientific Papers****Submission Status: Accepted****Contact:**

Lubomir Hadjiiski
University of Michigan

Phone: 734-647-7428
Fax: 734-615-5513
E-Mail: lhadjisk@umich.edu

Primary Category: Breast Imaging

Secondary Category: CAD

Thu Nov 29 2007 10:40AM - 10:50AM ROOM Arie Crown Theater**02) ROC Study: Computer-aided Diagnosis of Malignant and Benign Breast Clustered Microcalcifications in Temporal Pairs of Mammograms and Its Effect on Radiologists' Characterization Performance**

L M Hadjiiski, PhD, Ann Arbor, MI; P Filev, BS; H Chan, PhD; B Sahiner, PhD; M A Roubidoux, MD; M A Helvie, MD; et al. (lhadjisk@umich.edu)

PURPOSE

To evaluate the effects of computer-aided diagnosis (CAD) on radiologists' characterization of clustered microcalcifications on serial mammograms.

METHOD AND MATERIALS

We developed an automated CAD system to register and classify microcalcification clusters as malignant or benign based on interval change information on serial mammograms. In this study we improved the CAD system by designing new features and a neural network classifier for cluster analysis. An observer experiment using receiver operating characteristic (ROC) methodology was conducted to evaluate the effects of CAD on radiologists' estimates of the likelihood of malignancy (LM) and BI-RADS categories of the microcalcifications. 261 pairs of serial mammograms from 94 patients containing clustered microcalcifications (94 malignant and 167 benign) were chosen from patient files with IRB approval. The true cluster locations on current and prior mammograms were identified by an MQSA radiologist. For each cluster on current mammogram, the corresponding cluster on prior was automatically detected and matched with the current cluster. Cluster features were extracted and analyzed by the CAD system. All cases eventually underwent biopsy so that interval change was observed for most of the clusters even if they were found to be benign after biopsy. Eight MQSA radiologists read the temporal pairs that were displayed side-by-side on a workstation. The readers provided estimates of the LM and BI-RADS assessments without and then with CAD.

RESULTS

The CAD system alone achieved a test Az of 0.82 for this data set. For the 8 radiologists, the average Az in estimating the LM was 0.69 (range:0.63-0.73) without CAD and improved to 0.75 (range:0.68-0.82) with CAD. The improvement was statistically significant ($p=0.005$). Based on BI-RADS assessments the radiologists with CAD would perform 3.2% (3/94) more biopsies for malignant masses on average without increasing the number of biopsies for benign masses.

CONCLUSION

CAD using interval change analysis can significantly improve radiologists' accuracy in classification of clustered microcalcifications on serial mammograms.

CLINICAL RELEVANCE/APPLICATION

CAD using interval change analysis may increase the positive predictive value of mammography.

Disclosures:

No Disclosure:	Lubomir Hadjiiski
No Disclosure:	Peter Filev
No Disclosure:	Heang-Ping Chan
No Disclosure:	Berkman Sahiner
No Disclosure:	Marilyn Roubidoux
General Electric Company	Mark Helvie
No Disclosure:	Chintana Paramagul
No Disclosure:	Alexis Nees
No Disclosure:	Stephanie Patterson
No Disclosure:	Caroline Blane
No Disclosure:	Renee Pinsky
No Disclosure:	Annette Joe
No Disclosure:	Janet Bailey

Questions:

1. **Published email:** Do you wish to have an email address published in the RSNA program?

Yes

If yes, please provide one email address:

lhadjisk@umich.edu

2. **Disclosure of "Off-Label" usage:** The RSNA recognizes the authors may discuss the application of devices, materials, or pharmaceuticals that are not FDA approved for the discussed application. In keeping with the highest standards of professional integrity and ethics, the RSNA requires full disclosure of the discussion of the unlabeled use of a medical device, product, or pharmaceutical that has not been approved by FDA. Please mark the appropriate response below as to whether you or any of your co-authors will or will not describe the investigational or "Off-label" use of a medical device, product or pharmaceutical that is classified by the FDA as investigational for the intended use. If you or any of your co-authors will discuss or describe investigational or unlabeled products, the presenting author is responsible for disclosing the information to the audience.

No, I do not intend to discuss off-label uses

3. **SUBMISSION OF MANUSCRIPT** An important part of scientific progress is the timely publication of new research; also important is the thorough peer review of all manuscripts prior to acceptance for publication. (To view how to submit your manuscript, click on (Publications) under the above Help menu). Please tell us to which of the following journals you plan to submit your work (select one):

If you marked OTHER please indicate the name of the journal.

No response

4. **Digital Scientific Presentations:** (If your presentation is accepted) With the permission of the authors, RSNA will post digital scientific presentations on the Web for a maximum of one year after the RSNA annual meeting. RSNA scientific presentations posted on the Web are not considered prior publication by the editors of *Radiology* and *Medical Physics*. Thus the manuscript of your presentation will be considered for publication if you choose to submit it.

I give RSNA permission to record and post my presentation.

5. **Department Chair:** Beginning in 2006 RSNA provided department chairs a list of presentations from their institution. In order to ensure that your work is appropriately recognized, please provide the name of your department chair:

N. Reed Dunnick, MD

6. **Institution:** This work was primarily conducted at the following institution:

Department of Radiology, University of Michigan



Certificate of Merit

Citation to

Lubomir M. Hadjiiski; Heang-Ping Chan;
Berkman Sahiner; Alexis V. Nees; Janet E.
Bailey; Stephanie K. Patterson; et al

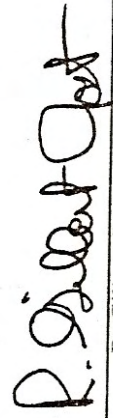
In recognition of the excellence of your

Education Exhibit

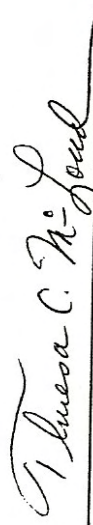
LL-PH5155: Computer-aided Characterization of Malignant and Benign Breast Clustered
Microcalcifications on Serial Mammograms: Early Experience of Its Effects on Radiologists'
Performance from an ROC Study

presented at the
92nd Scientific Assembly and Annual Meeting of the
Radiological Society of North America

November 26 - December 1, 2006


R. Gilbert Jost, MD
President




Theresa C. McLoud, MD
President-elect and Secretary/Treasurer